REPORT DOCUMENTATION PAGE

Form Approved OMB NO. 0704-0188

1. REPORT DATE (DD-MM-YYYY)	2. REPORT TYPE	3. DATES COVERED (From - To)
25-11-2018	Final Report	15-Oct-2013 - 30-Jun-2017

4. TITLE AND SUBTITLE
Final Report: Ultrafast Carbon Nanotube-Oxide-Metal Tunnel Diodes for Infrared and Optical Rectenna: A Study of the Limiting Resistances

5a. CONTRACT NUMBER
W911NF-13-1-0491

5b. GRANT NUMBER

5c. PROGRAM ELEMENT NUMBER
611102

6. AUTHORS

5d. PROJECT NUMBER

5e. TASK NUMBER

5f. WORK UNIT NUMBER

7. PERFORMING ORGANIZATION NAMES AND ADDRESSES
Georgia Tech Research Corporation
505 Tenth Street NW

Atlanta, GA 30332 -0420

8. PERFORMING ORGANIZATION REPORT NUMBER

9. SPONSORING/MONITORING AGENCY NAME(S) AND ADDRESS (ES)
U.S. Army Research Office
P.O. Box 12211
Research Triangle Park, NC 27709-2211

10. SPONSOR/MONITOR'S ACRONYM(S)
ARO

11. SPONSOR/MONITOR'S REPORT NUMBER(S)
64600-EL-YIP.3

12. DISTRIBUTION AVAILIBILITY STATEMENT
Approved for public release; distribution is unlimited.

13. SUPPLEMENTARY NOTES
The views, opinions and/or findings contained in this report are those of the author(s) and should not contrued as an official Department of the Army position, policy or decision, unless so designated by other documentation.

14. ABSTRACT

15. SUBJECT TERMS

16. SECURITY CLASSIFICATION OF:			17. LIMITATION OF ABSTRACT	15. NUMBER OF PAGES	19a. NAME OF RESPONSIBLE PERSON
a. REPORT	b. ABSTRACT	c. THIS PAGE			Baratunde Cola
UU	UU	UU	UU		19b. TELEPHONE NUMBER 404-385-8652

RPPR Final Report
as of 26-Nov-2018

Agency Code:

Proposal Number: 64600ELYIP **Agreement Number: W911NF-13-1-0491**
INVESTIGATOR(S):

Name: Baratunde A. Cola
Email: cola@gatech.edu
Phone Number: 4043858652
Principal: Y

Organization: **Georgia Tech Research Corporation**
Address: 505 Tenth Street NW, Atlanta, GA 303320420
Country: USA
DUNS Number: 097394084 EIN: 580603146
Report Date: 30-Sep-2017 Date Received: 25-Nov-2018
Final Report for Period Beginning 15-Oct-2013 and Ending 30-Jun-2017
Title: Ultrafast Carbon Nanotube-Oxide-Metal Tunnel Diodes for Infrared and Optical Rectenna: A Study of the Limiting Resistances
Begin Performance Period: 15-Oct-2013 **End Performance Period:** 30-Jun-2017
Report Term: 0-Other
Submitted By: Baratunde Cola Email: cola@gatech.edu
Phone: (404) 385-8652
Distribution Statement: 1-Approved for public release; distribution is unlimited.

STEM Degrees: 1 **STEM Participants:** 2

Major Goals: We will carry out in depth experimental investigations of electronic properties of interfaces and resistances in CNT-O-M architectures. Our studies will address the following open scientific questions:
(a) What are the limits on how thin an oxide barrier can be in a CNT-O-M diode structure as determined by fabrication limits and fundamental limits on diode operation by quantum mechanical tunneling? How are these limits affected by temperature?
(b) What roles do CNT-oxide or oxide-metal interfaces play in controlling the barrier heights and tuning the rectification ratio at infrared and optical frequencies?
(c) What is the lowest series resistance that can be achieved in a single multiwall CNT-O-M diode junction?
Motivated by these fundamental scientific questions and to lay the foundation for developing new devices using the unique electronic and electromagnetic properties of CNTs, the objectives of this research program are to:
(1) Determine the limit of CNT diode oxide insulator thickness dictated by fabrication limits. Our preliminary experiments suggest that the thickness of the oxide insulator layer affects the barrier height and consequently correlates to the turn on voltage and tunneling current. With improved fabrication procedures such as CNT functionalization to improve oxide nucleation density we aim to test the lower limit of insulator thickness and fundamental limits on diode operation by quantum mechanical tunneling.
(2) Develop an approach to make electrical contact to the inner walls of multiwall CNTs in the diode junctions. Our preliminary experiments suggest that the series resistance of a single CNT diode junction is at least 20 G?, which is about eight orders of magnitude higher than what has been achieved for ohmic contacts to open-ended multiwall CNTs [2]. Nanofabrication techniques will be employed to open the ends of CNTs in the diode junctions to facilitate low resistance contacts and conduction through multiple multiwall CNT shells to quantify and understand the achievable lower limit to single junction series resistance.
(3) Discover the physics of CNT-oxide and oxide-metal barrier heights optimized for low resistance and high asymmetry. One possible way to lower the resistance and turn-on voltage, and maximize asymmetry and nonlinearity is to bring the electron affinity of the insulator close to the value of one of the electrode work functions so as to produce low barrier height. We will investigate the interface electronic barrier height to engineer the electronic structure at the interfaces. We will modify the electronic structure of the CNTs by introducing donor or acceptor levels (N or B) through doping to understand the effects of doping on diode performance and rectenna efficiency. Such dopants can introduce acceptor like or donor like states very close to the Fermi level (within 0.5 eV) of the CNTs because of the formation of nanodomains in the lattice. Oxide materials (Al2O3, ZrO2, TiO2) with different electron affinity (1.0, 2.5 and 3.9 eV) will be studied as a means to tune the barrier level at the CNT-oxide and oxide-metal interfaces. The effect of the work function of the contact metals on diode asymmetry and nonlinearity will also be explored.

RPPR Final Report
as of 26-Nov-2018

We will accomplish our objectives with controlled materials processing and characterization, and by cross correlating experimentally measured responses to electromagnetic irradiation with various electrical device parameters such as capacitance, resistance, reactance, etc., and electronic parameters such as experimentally determined barrier heights at CNT-O, and O-metal interfaces. These scientific investigations will also improve our overall understanding of nanostructures and oxide interfaces that could potentially be applied to other M-O-M device architectures for similar applications or to other material systems such as nanowires, or polymer nanostructures for applications in energy storage or harvesting devices. Therefore, our proposed research will offer a unique opportunity to further establish the scientific relevance and potentially transformative impact of nanostructures and oxide interfaces in a variety of applications for unique strategic and economic relevance to the US Army and other US defense and private sector enterprises.

Accomplishments: See attached in upload section

Training Opportunities: A masters student, 1 Ph.D. student, and a visiting professor gained the opportunity to work on carbon nanotube optical rectenna as a result of this grant. The training included fabrication, characterization, and modeling.

Results Dissemination: The PI gave 5 invited seminars and talks directly related to sharing the results of this program.

We published the below in prestigious journals.

High Performance Multiwall Carbon Nanotube–Insulator–Metal Tunnel Diode Arrays for Optical Rectification was published in 2018 (https://onlinelibrary.wiley.com/doi/full/10.1002/aelm.201700446)

A Carbon Nanotube Optical Rectenna was published in 2015 (https://www.nature.com/articles/nnano.2015.220)

Honors and Awards: PI Cola
ASME Bergles-Rohsenow Young Investigator Award in Heat Transfer (2015)
Georgia Tech Sigma Xi Faculty Best Paper Award (2016)
Woodruff Faculty Fellow (2016)
NSF Alan T. Waterman Award (2017)
AAAS Fellow (2017)

Graduate Student Erik Anderson
NSF Graduate Research Fellowship 2016

Protocol Activity Status:

Technology Transfer: Nothing to Report

PARTICIPANTS:

Participant Type: PD/PI
Participant: Baratunde Cola
Person Months Worked: 1.00 **Funding Support:**
Project Contribution:
International Collaboration:
International Travel:
National Academy Member: N
Other Collaborators:

Participant Type: Graduate Student (research assistant)
Participant: Erik Anderson
Person Months Worked: 1.00 **Funding Support:**
Project Contribution:

International Collaboration:
International Travel:
National Academy Member: N
Other Collaborators:

Summary of Rectenna Results

NEST Lab

Georgia Institute of Technology

Navigation

One-Slide Summary

- Al vs Ag Device Comparison
  - Ag found to be better top metal for all choices of oxide: higher current density and lower resistance.
- Ca(40nm)-Al(20nm) Device
  - 30 sec RIE to open tips gave consistently higher current
  - Lower oxide thicknesses gave higher current and lower resistance, but lower asymmetry
  - After 5 days of letting Ca fully oxidize: current density was lower, resistance was higher, and asymmetry was higher.
  - Overall need for a way to control Ca oxidation

I-V Characteristics of Aluminum or Silver as Rectenna Device Top Metal

Parameters studied:

- Ag vs Al top metal
- 3 to 8 nm oxide thickness

- Device fabrication:
  - 150/10/3 nm Ti/Al/Fe catalyst layer
  - CNT growth for 180 sec: ~10um height
  - 3, 5, or 8 nm oxide layer
  - 50nm either Al or Ag top metal

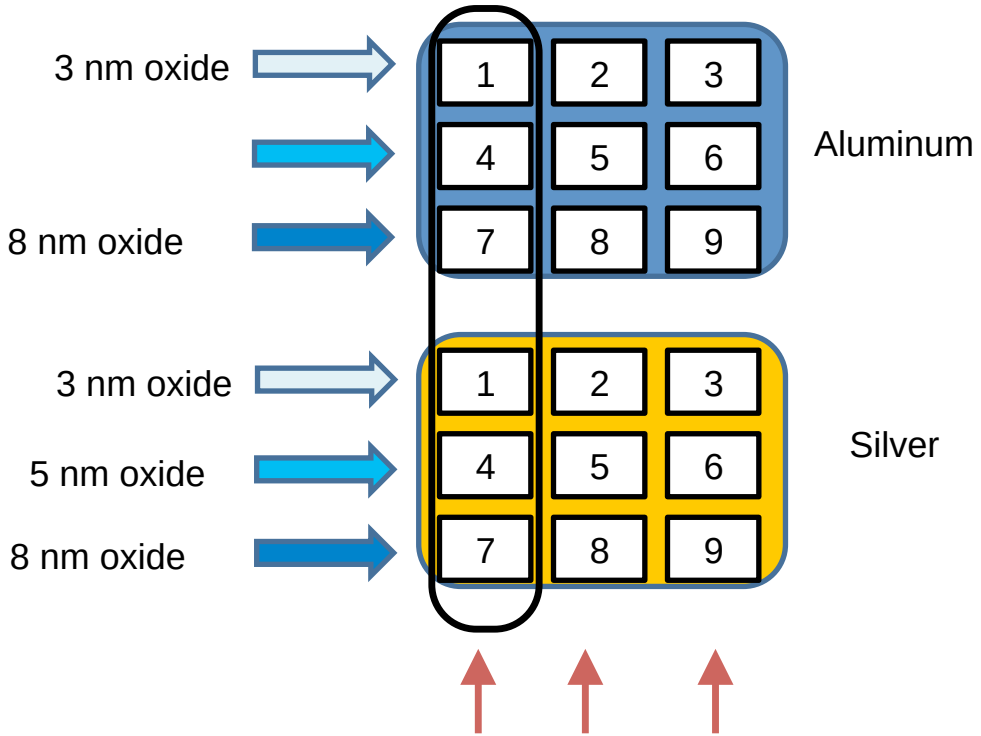

This is our sample numbering scheme, just to make sure it was clear which sample we were testing.
There are 3 samples for each oxide-metal combination, taken from 3 different runs of catalyst deposition (to test the reliability of the deposition).

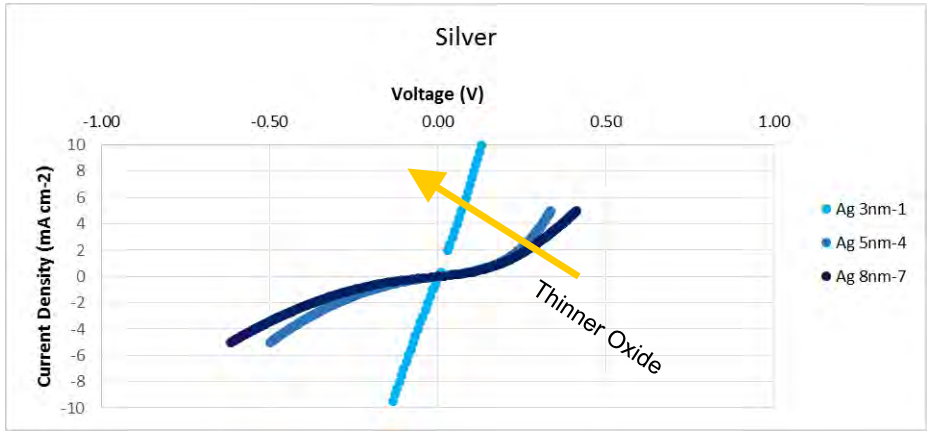

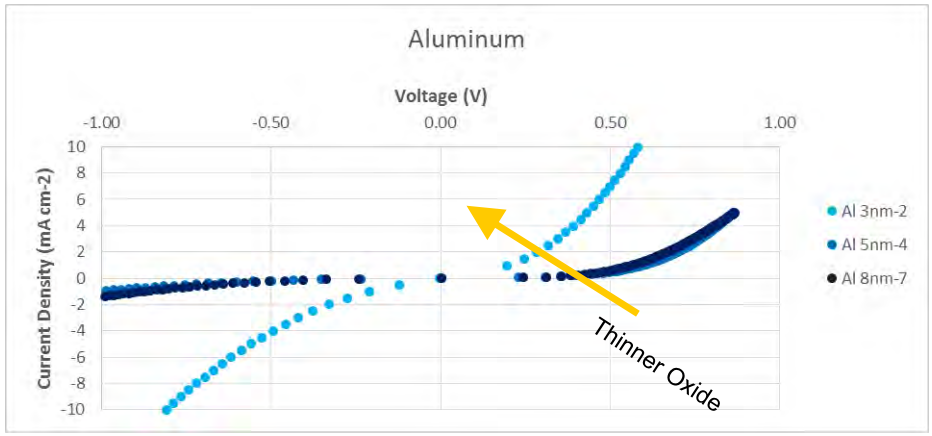

- Results:
  - Thinner oxide thickness yielded greater current density, though at the cost of less asymmetry and nonlinearity
  - Silver seemed to perform better than aluminum

Resistance

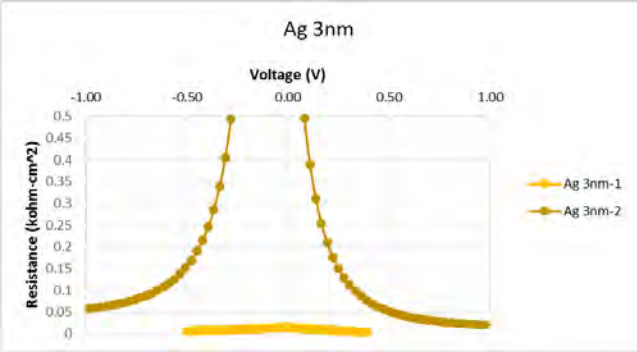

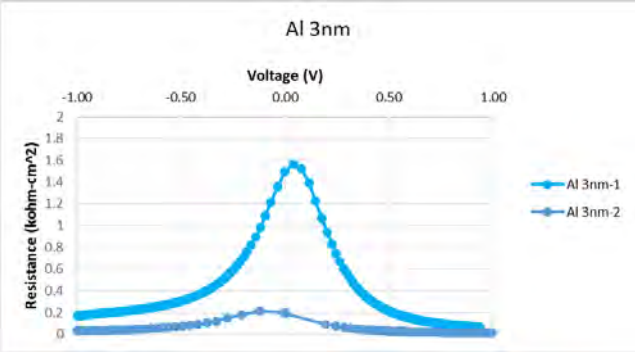

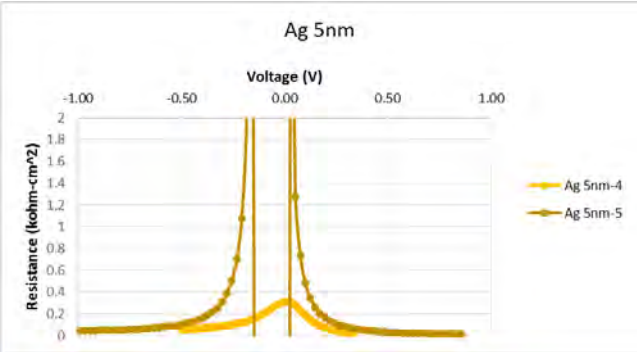

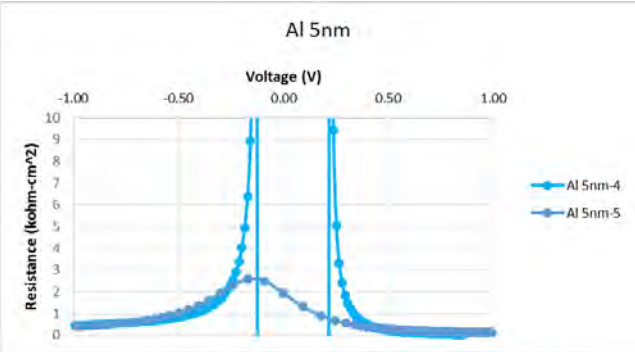

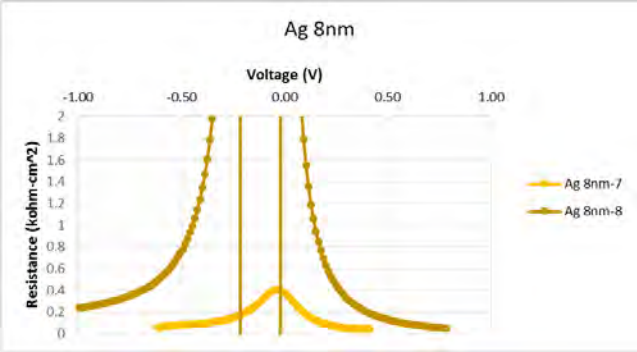

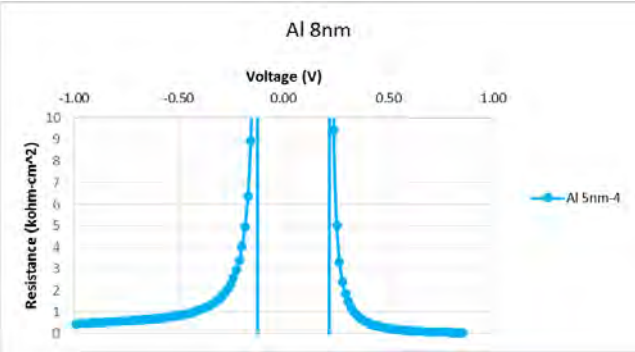

- 2 devices for each combination, taken from 2 separate fabrication runs
  - It is clear that one fabrication run did not produce effective devices
- Results:
  - Resistance is lower for silver than aluminum
  - Resistance increases with oxide thickness

Zero Bias Resistance

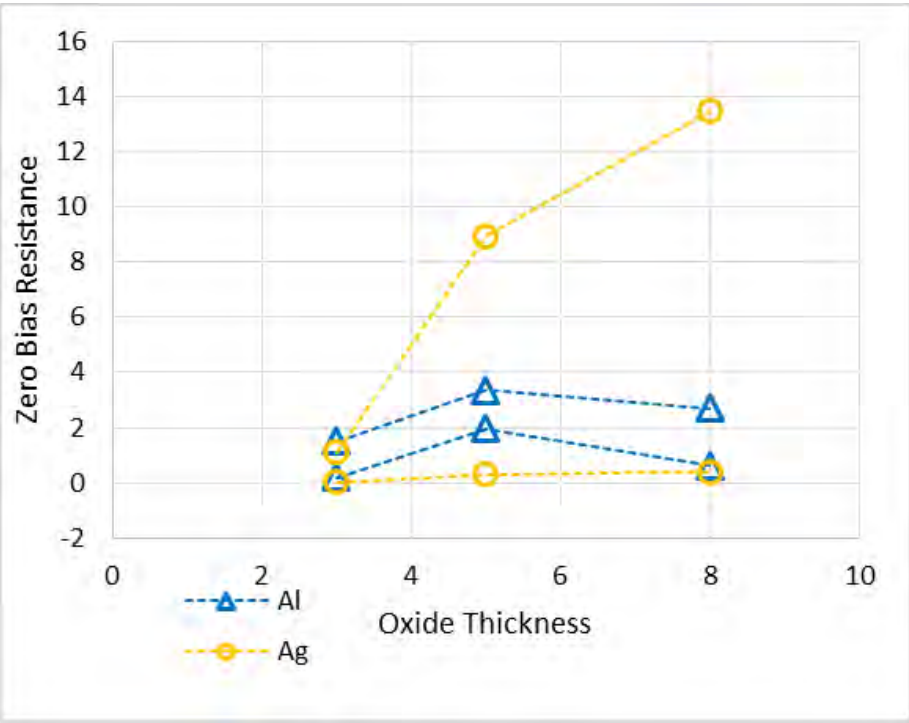

There is variation between two sets of silver samples (the two orange lines which represent two different catalyst deposition dates).
One set of Ag shows consistently lower zero bias resistance than Al.

Asymmetry

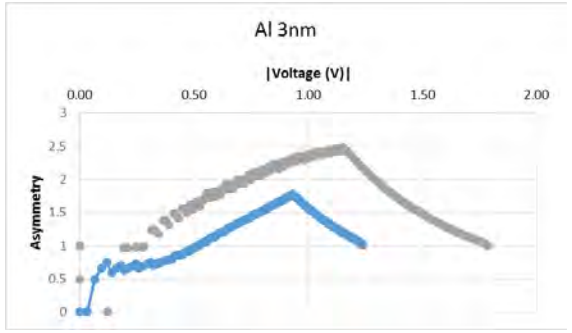

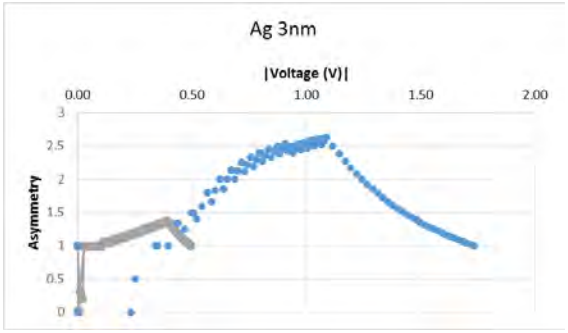

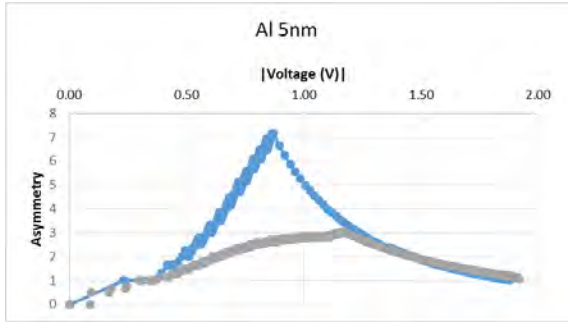

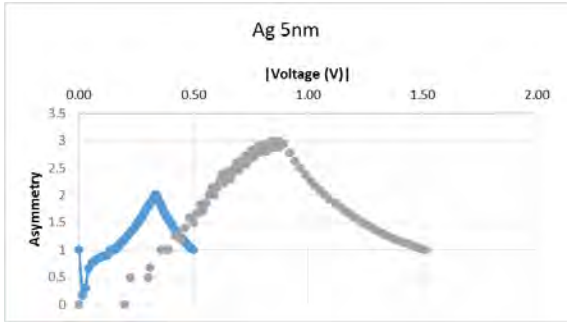

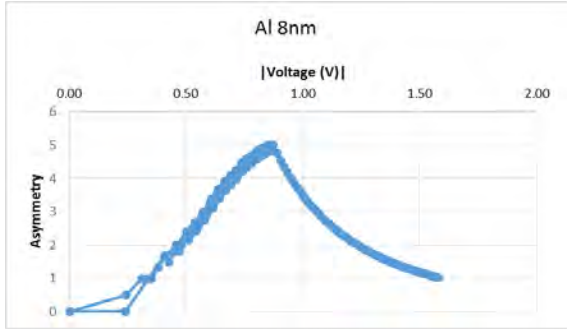

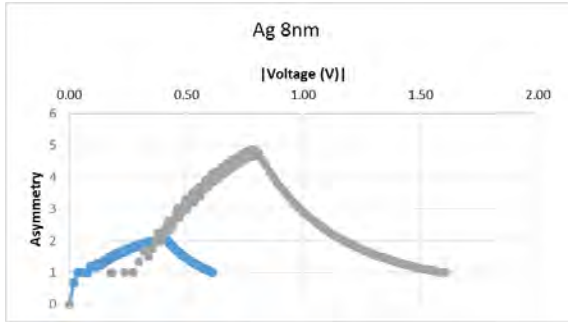

- Variation between two sample sets
- Results
  - Silver and aluminum showed similar asymmetry, considering the variation between fabrication runs

Conclusions

- Silver was shown to have consistently better properties than aluminum for use as a top metal
  - Higher current density
  - Lower resistance, including zero bias Resistance (though there was significant variations between fabrication runs)
  - Asymmetry was about similar

I-V Characteristics of Ca(40nm)-Ag(20nm)

Parameters studied:

- Ca(40nm)-Ag(20nm) layered top metal
- 2-8 nm oxide
- Open vs closed CNT tips

Summary of Devices

- Ca (40nm) with Ag (20nm) as top metal material
- 2, 4, 6, 8 nm Al_2O_3 oxide thicknesses
- 30 sec RIE etching vs. no etching

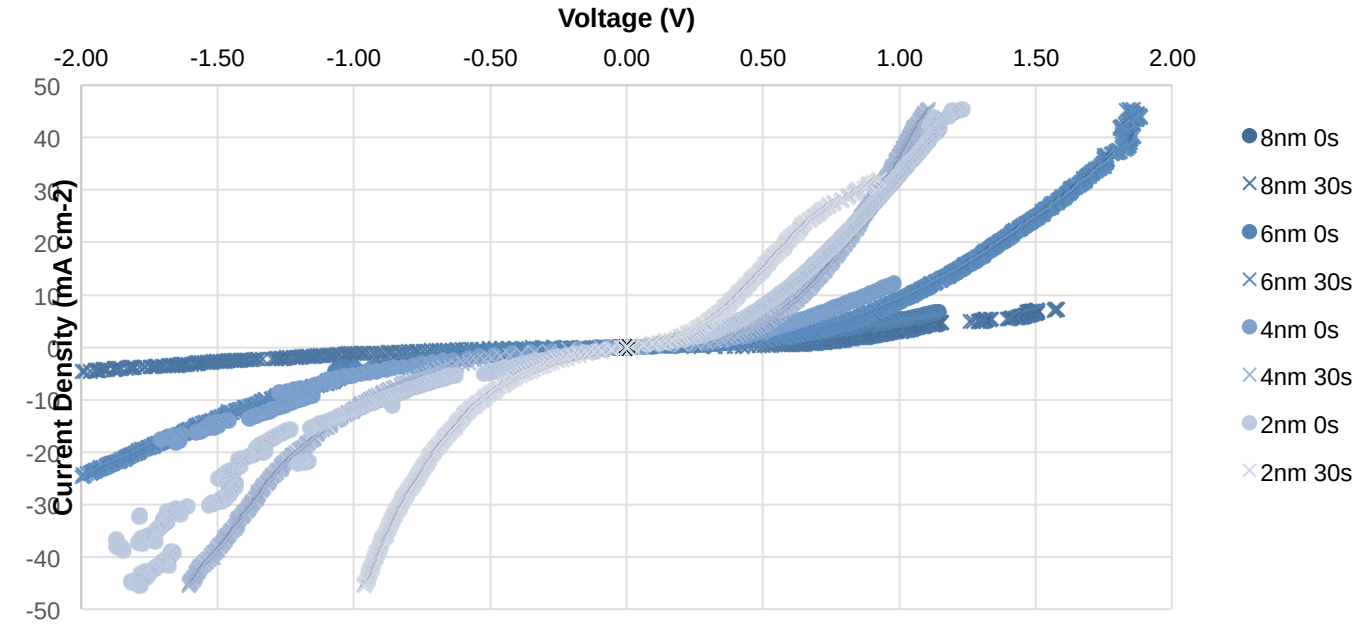

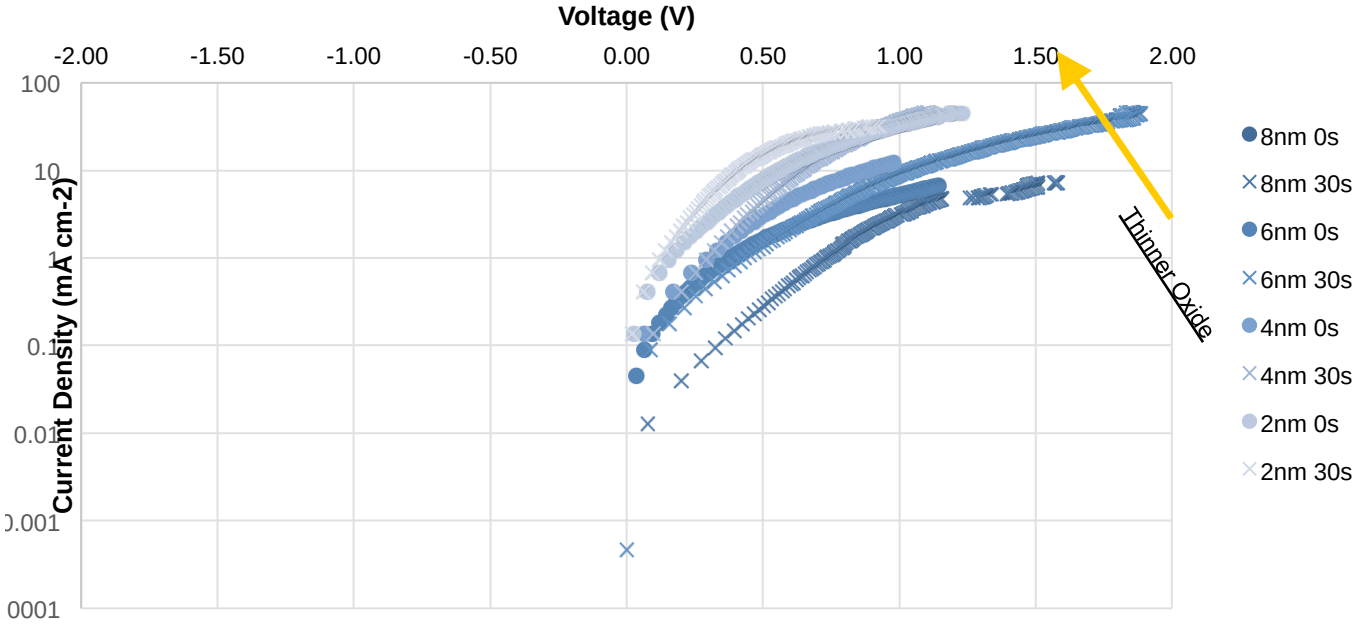

- Results:
  - Thinner Al2O3 oxide layer increased current
  - Slight, but consistent increase in current due to RIE

Resistance

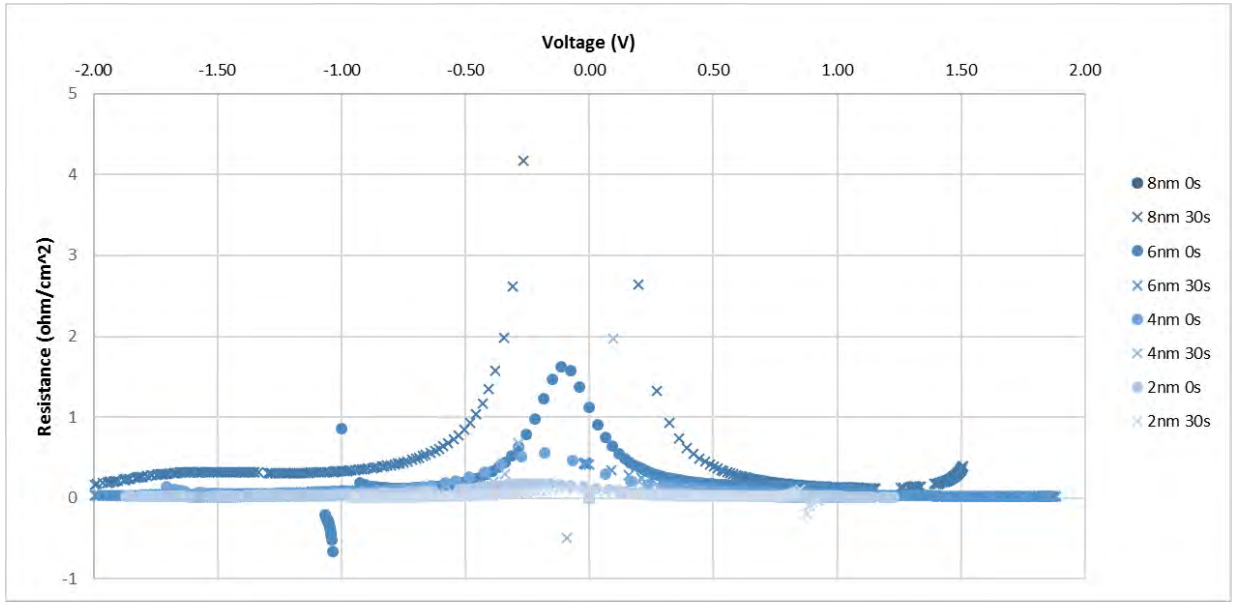

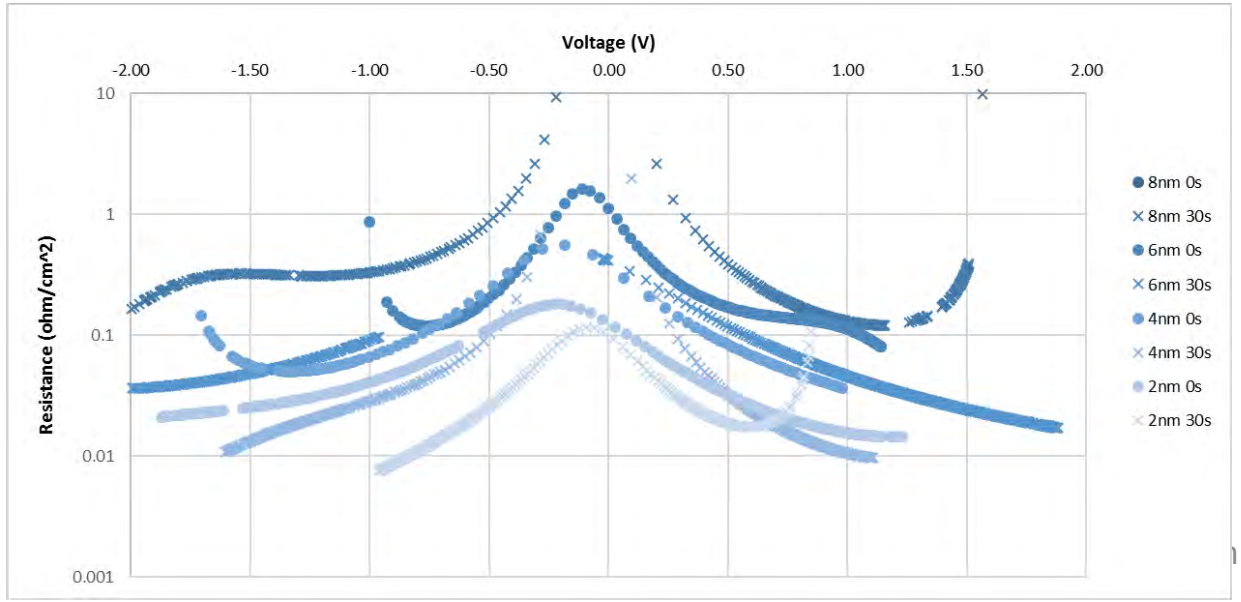

- Higher R with thicker oxide
- Consistently lower R with 30s RIE

Responsivity

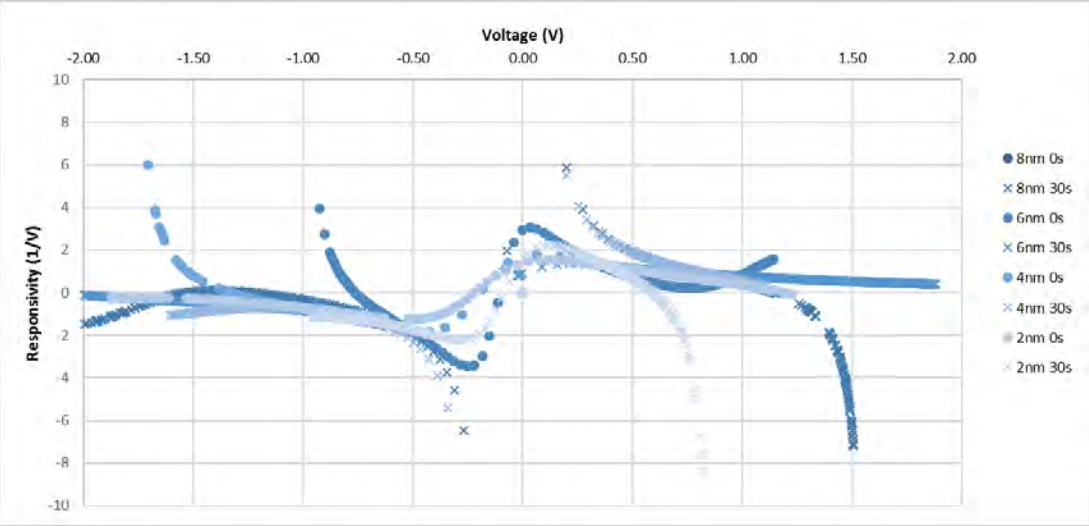

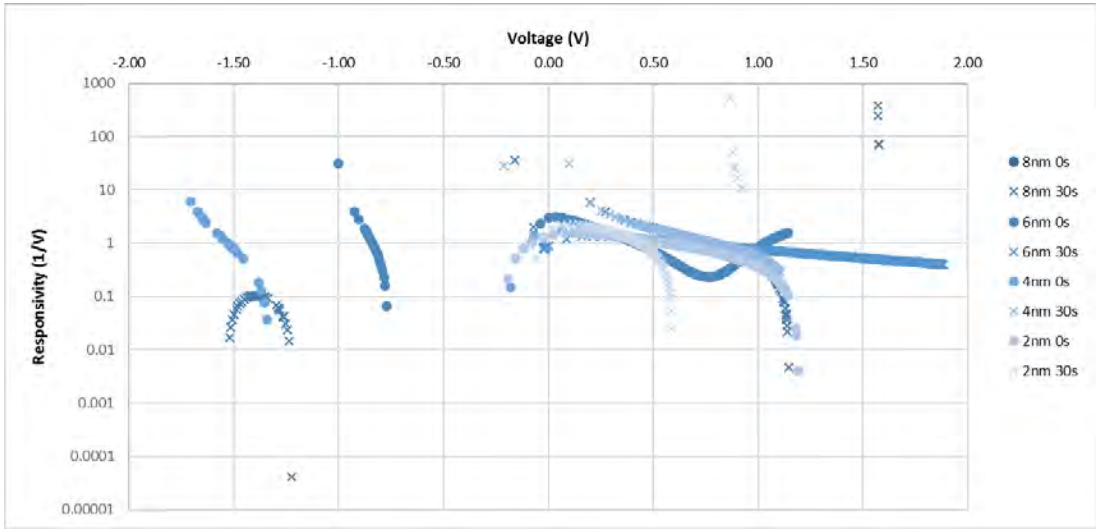

- Inconsistencies with the polynomial curve fitting approach makes responsivity curves unreliable and suspect. In the future, it would be better to linearly interpolate results

Asymmetry

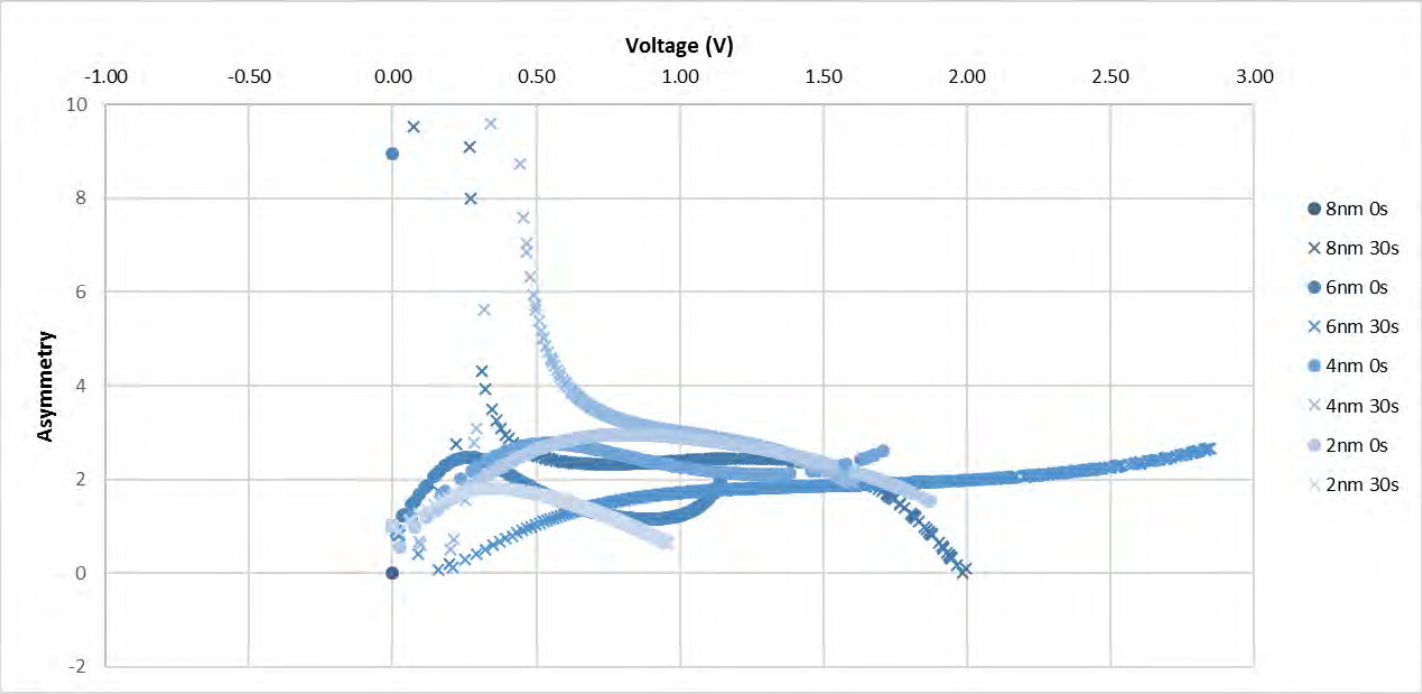

- No clear pattern with Asymmetry
- Although for the most part asymmetry is low: ~2-3

Comparison to 5 days oxidized

- Purpose was to check whether Ca had fully oxidized during the previously stated measurements
- Only performed on 0s RIE

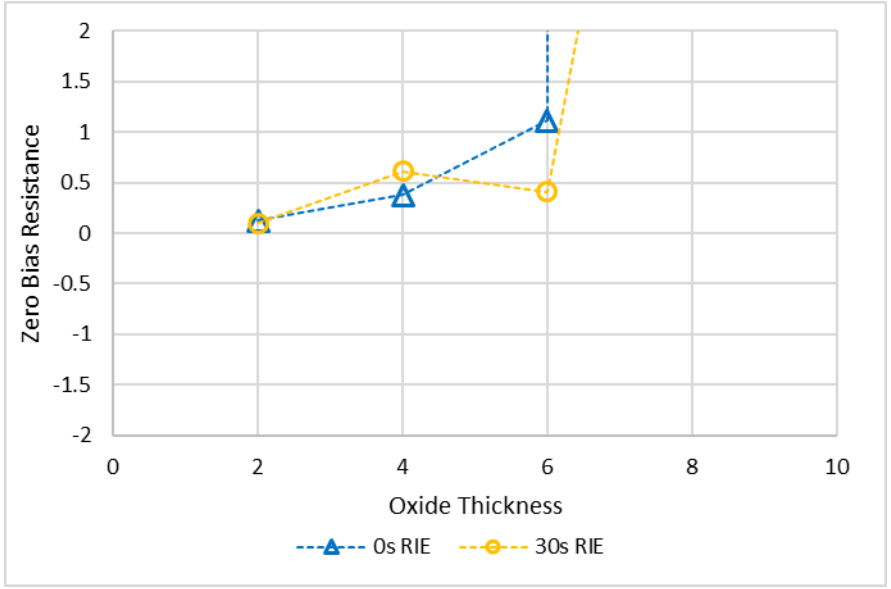

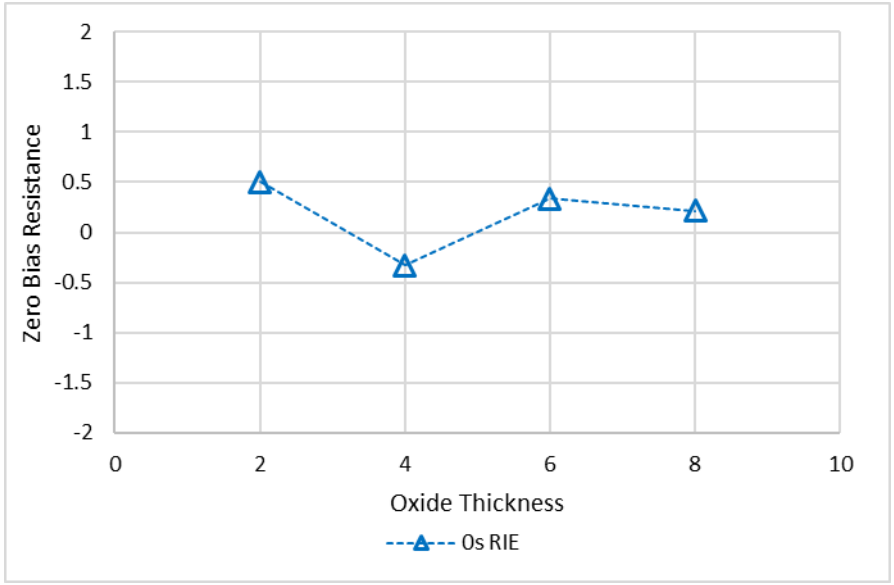

Current density lower (somewhat) with oxidation

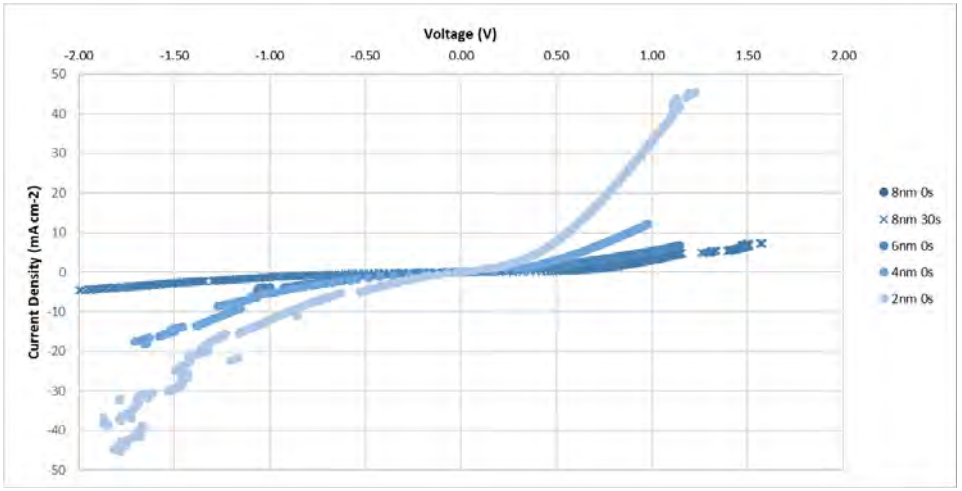

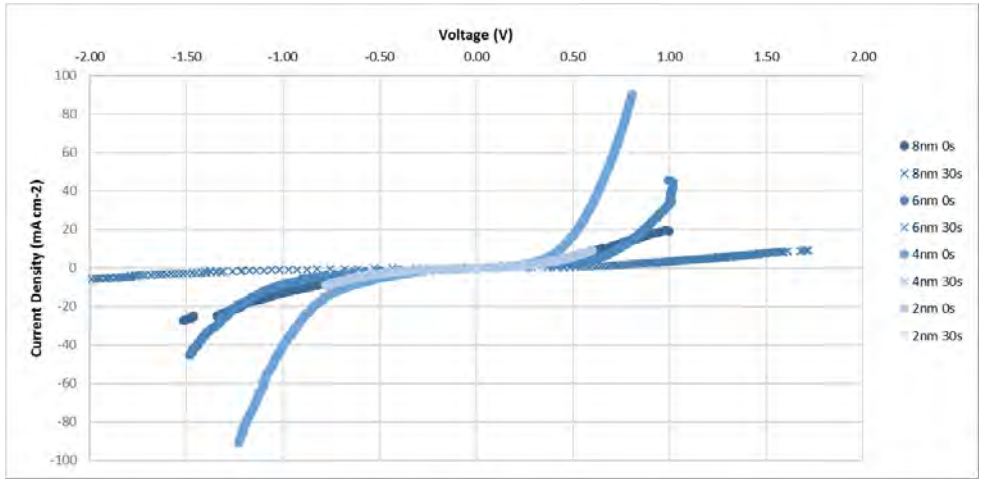

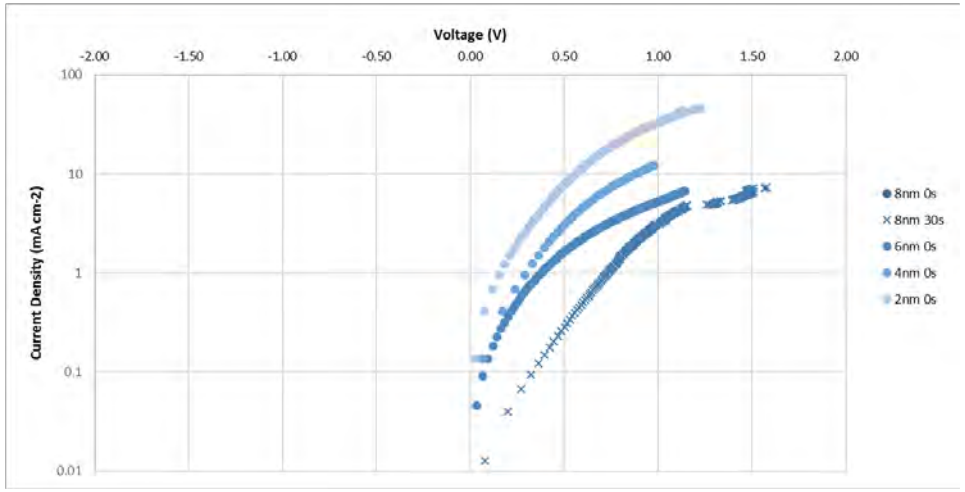

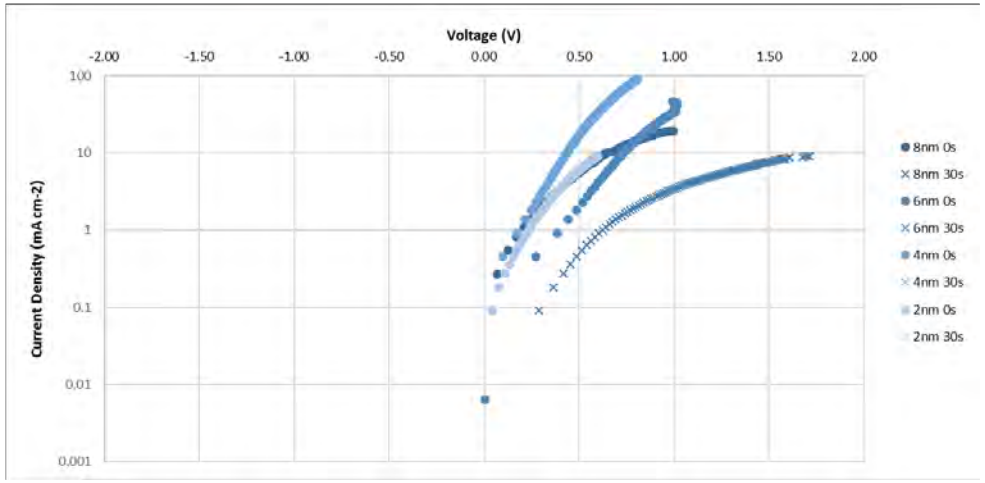

Resistance increases with oxidation

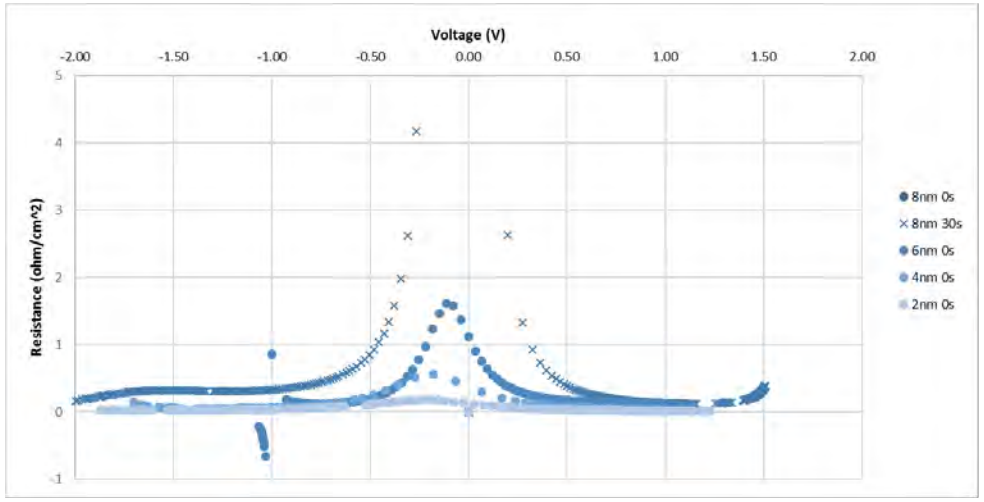

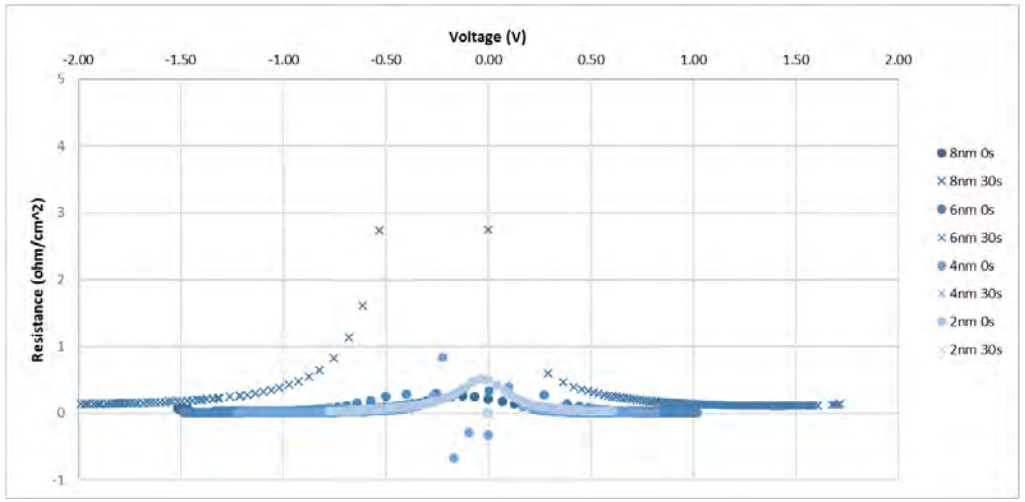

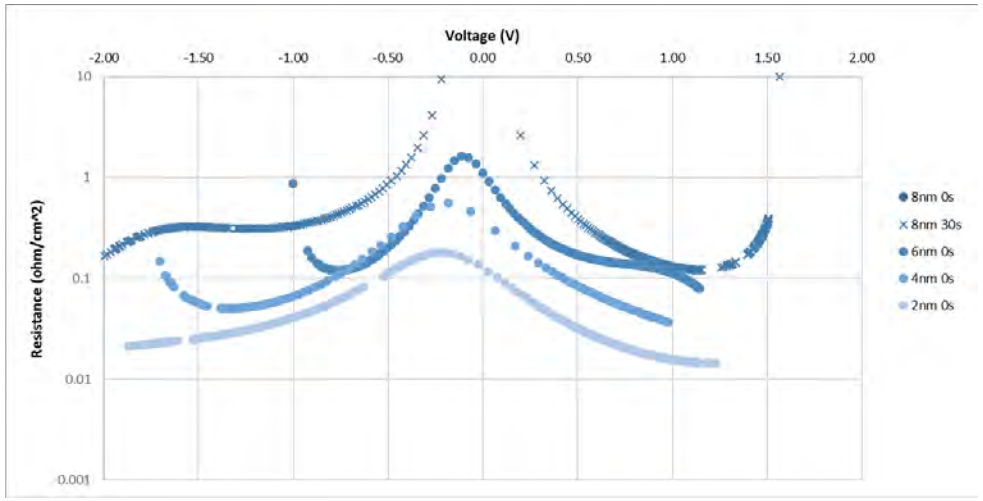

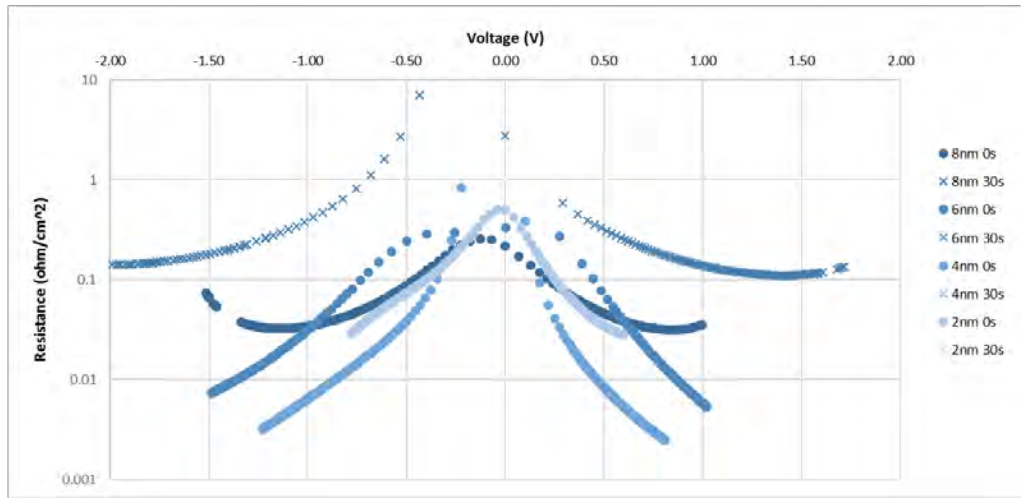

Asymmetry goes up with oxidation

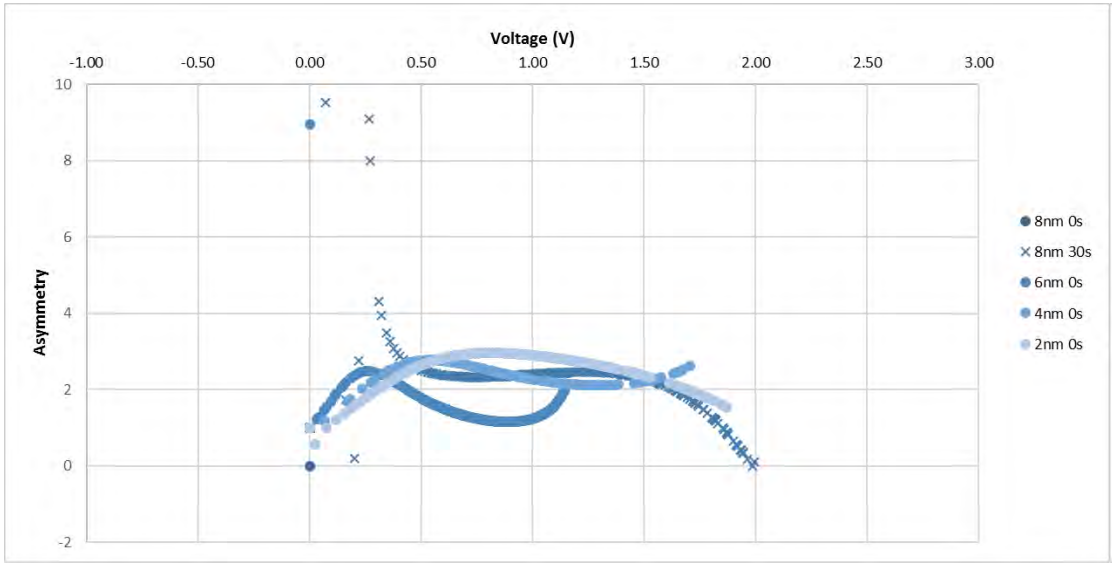

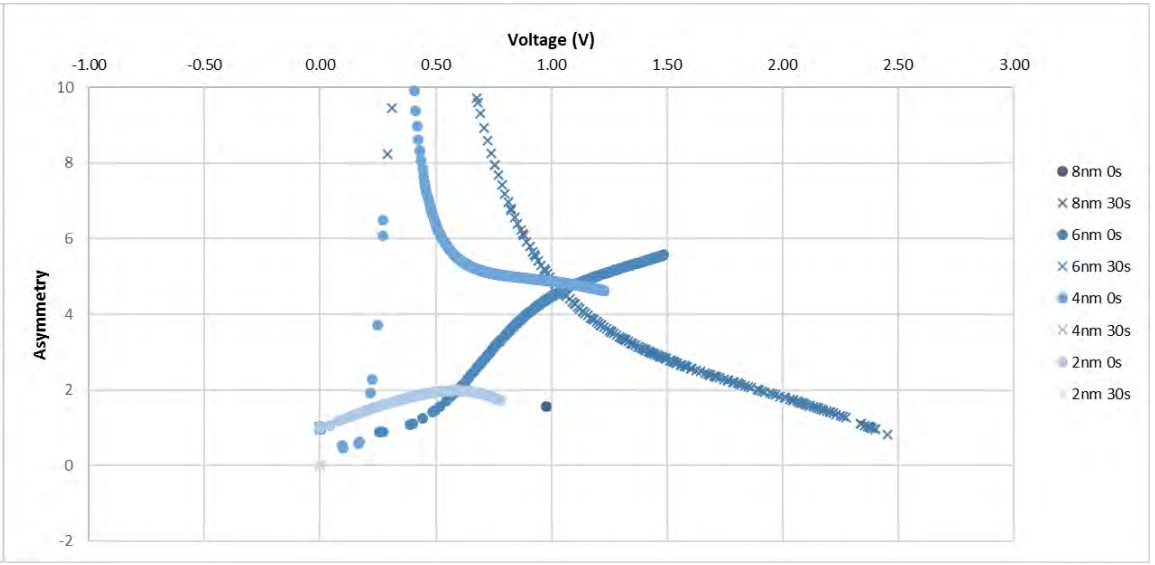

Conclusions of Ca-Ag devices

- Thinner oxide layer yield higher current and lower resistance, but suffers from somewhat lower asymmetry
- 30sec RIE gives consistent improvements to current density
- After 5 days of letting Ca sit in the open air, measurements showed variation from before, suggesting that the devices did not immediately oxidize during the first set of measurements
  - After Ca was fully oxidized: current density was lower, resistance was higher, and asymmetry was higher.
- Therefore, in the future we need a way to control the oxidation of Ca since that will end up altering results.

SEM Images of Ca-Ag Rectenna Device

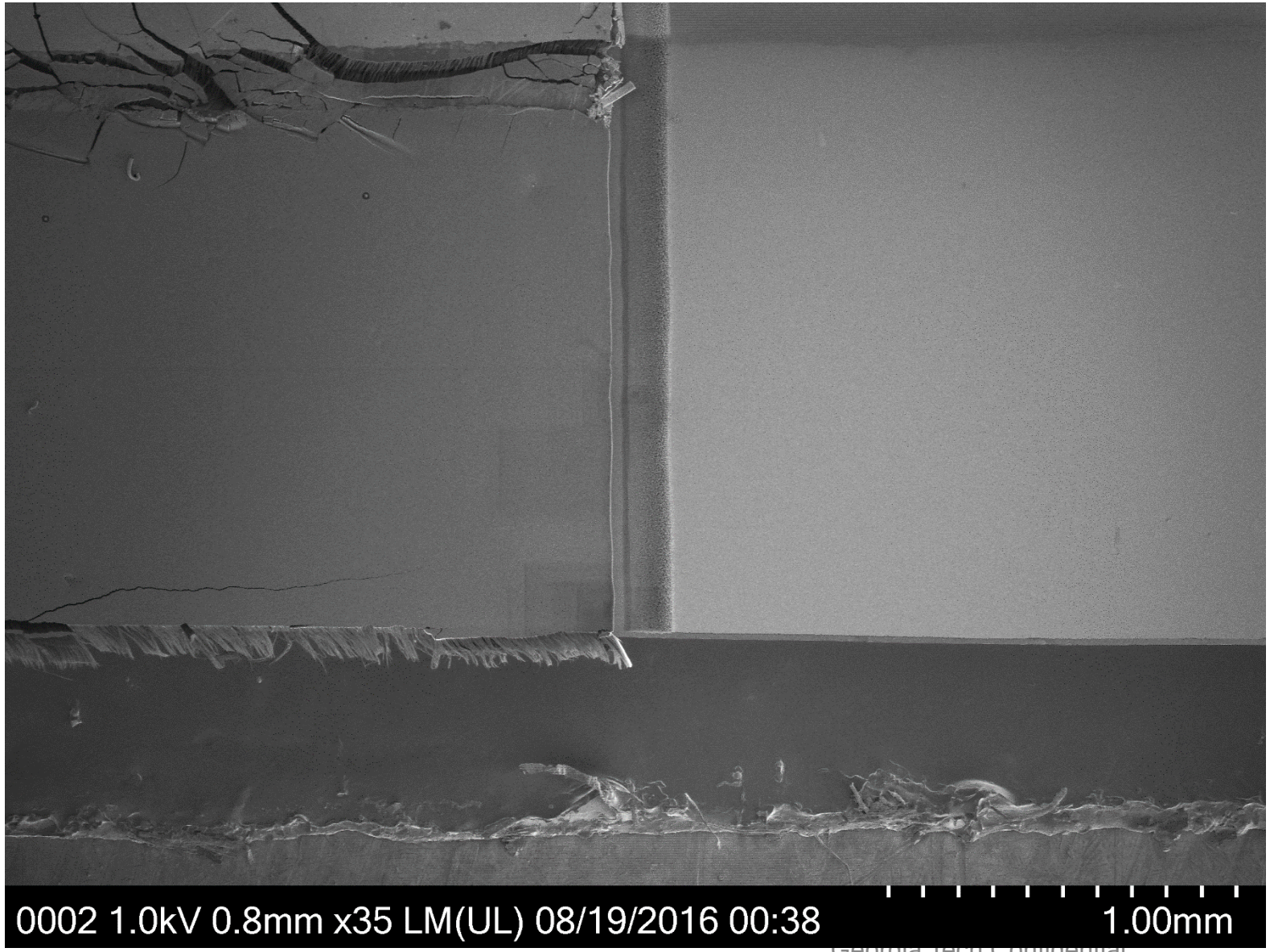

- Metal-on-CNT device fingers

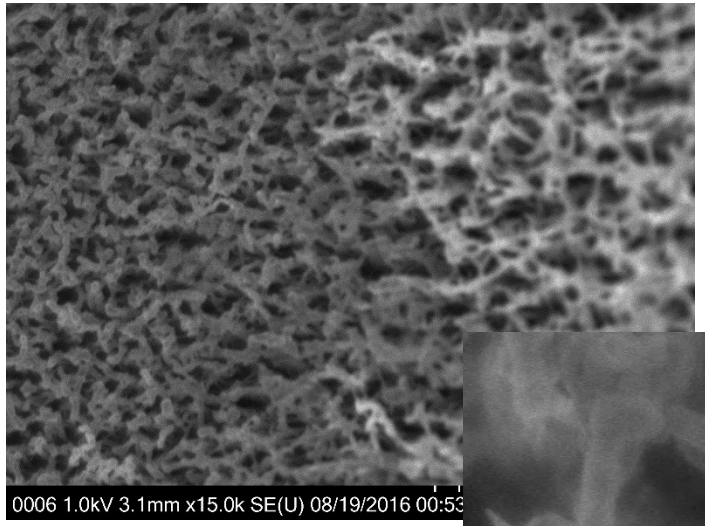

Shows that the CNTs are clearly coated in top metal

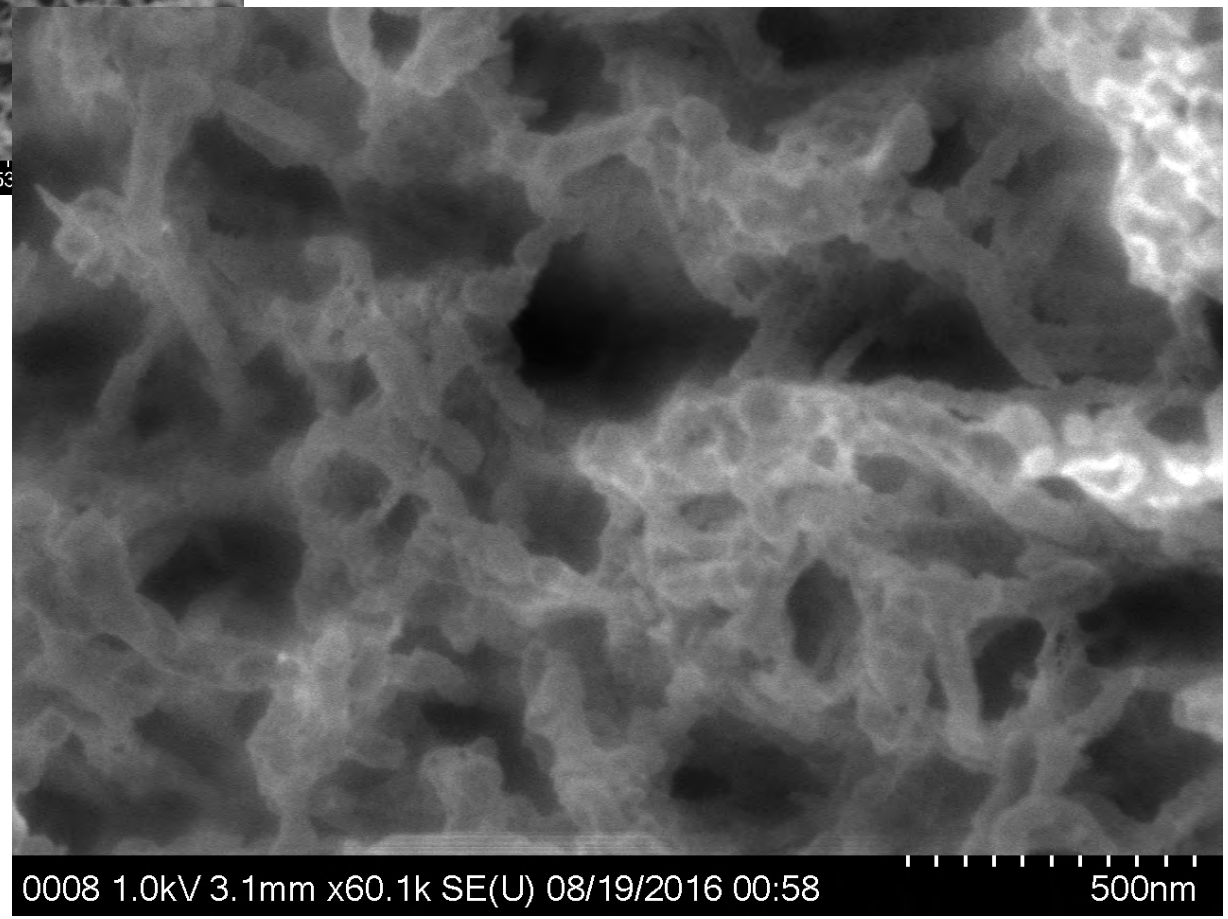

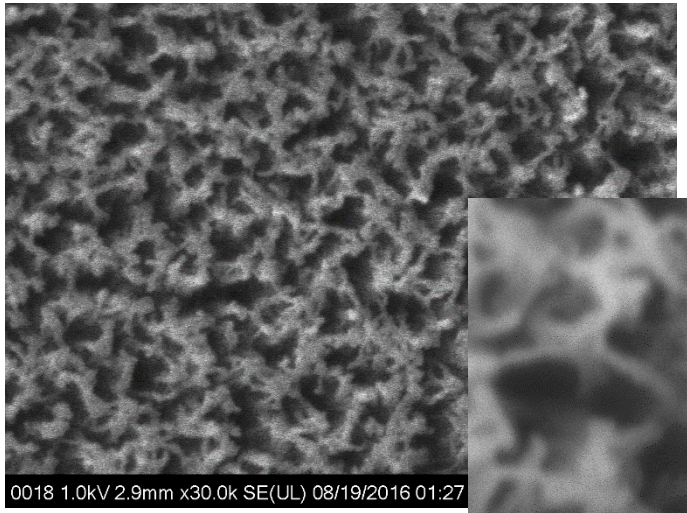

- Bare CNTs
(no top metal)

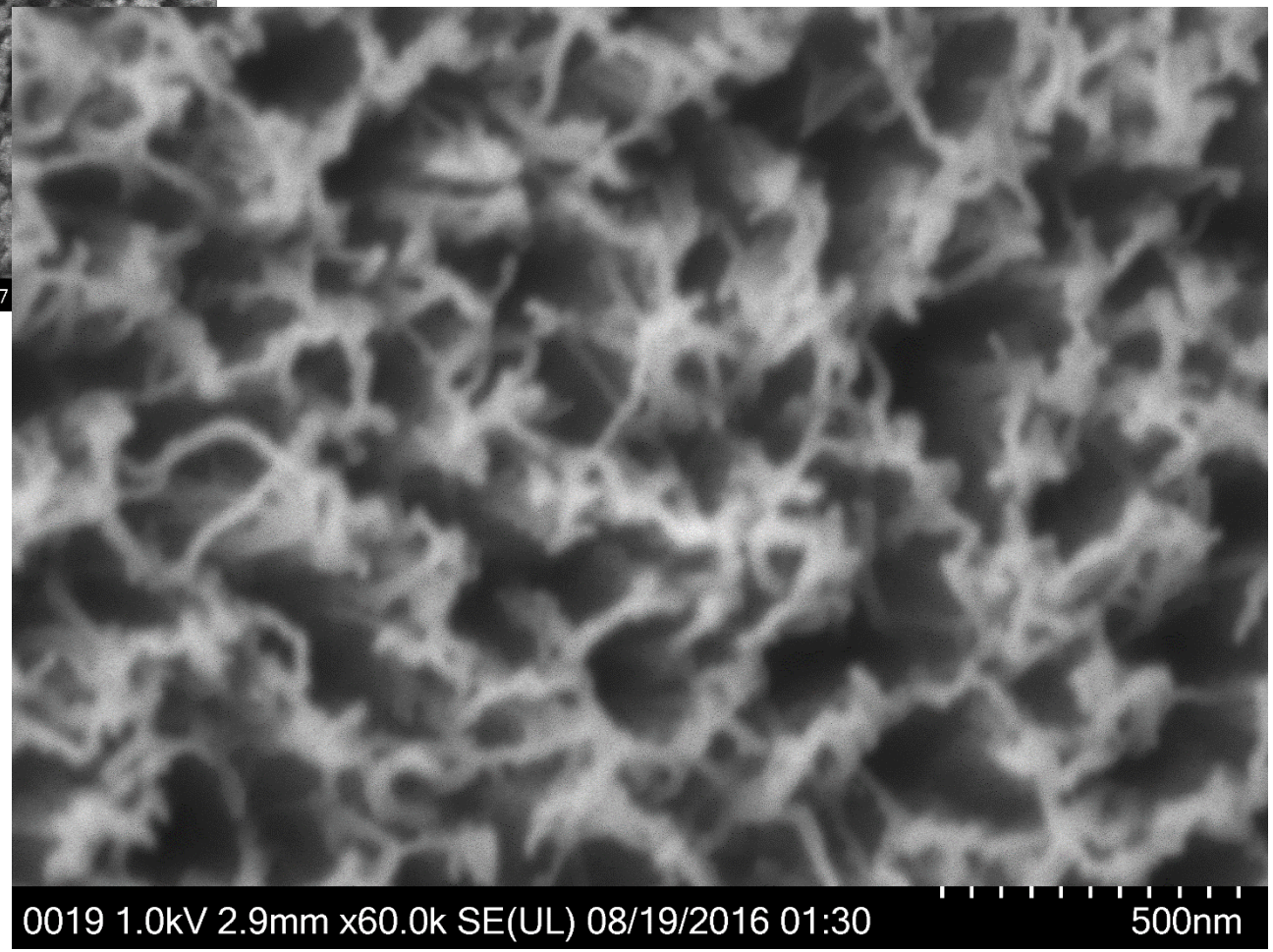

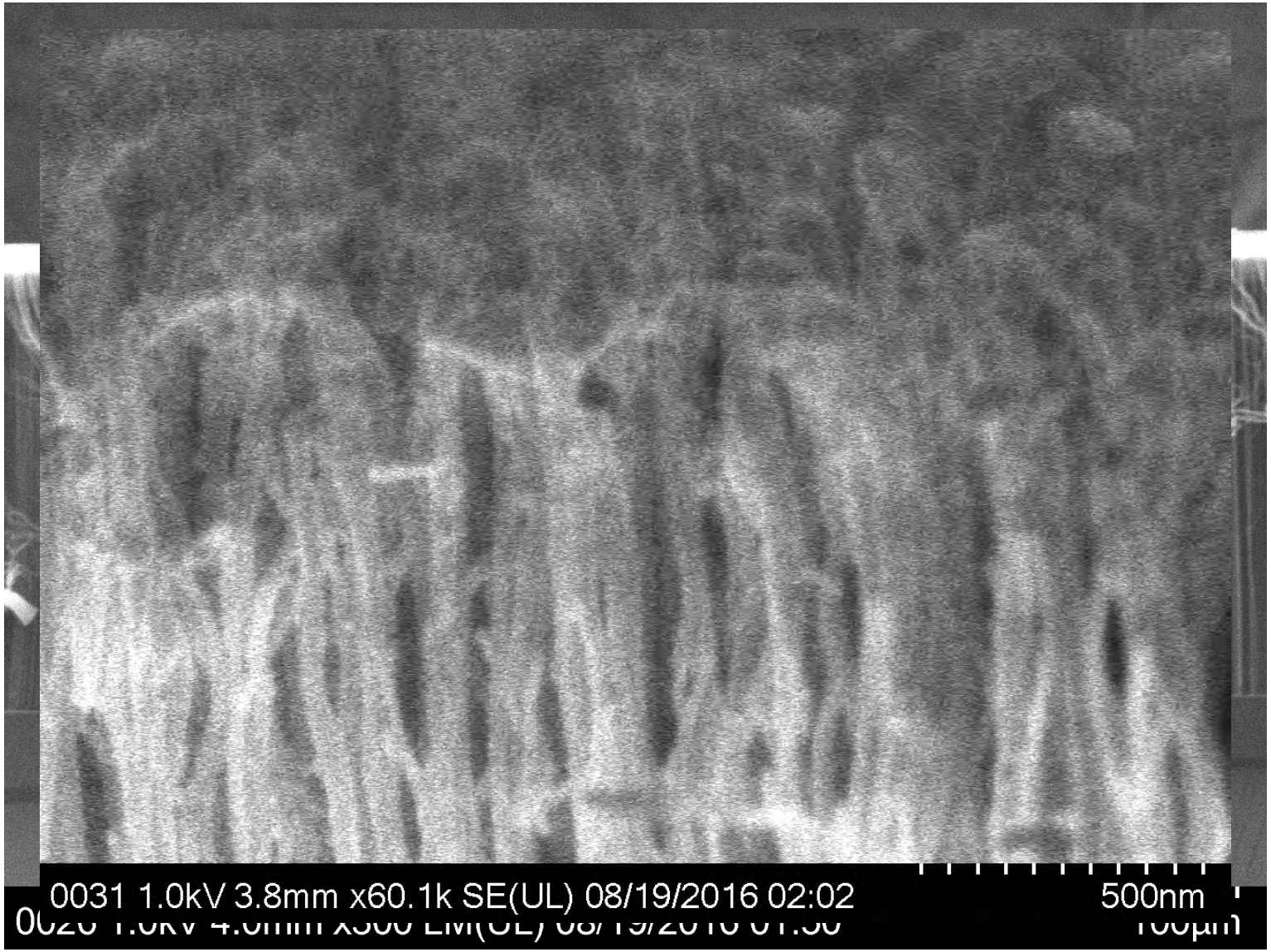

Shows that the top metal does not penetrate into the forest past 5-10um to coat the lower parts of the CNTs

Interim Report for Rectenna Project
GT Principal Investigator: Dr. Baratunde Cola
Date Submitted: August 31, 2015

Introduction:

Carbon nanotubes (CNTs) are promising candidates in electronics applications such as interconnects, diodes, transistors, sensors, rectenna, etc. due to their unique electrical properties. Multiwall CNTs (MWCNTs) have been shown to exhibit ballistic transport of charge carriers and possess exceptional electrical conductivity (1.85×10^3 S cm^{-1}) [1]. The electrical conduction occurs primarily in the in-plane direction of cylindrical graphene sheets concentric to the tube axis. Current densities approaching 10^9 A cm^{-2} have also been reported [2]. Coupled with their robust mechanical properties, this makes them a strong candidate as interconnects for microelectronic devices and electrodes in numerous applications. Growth of arrays of vertically aligned MWCNTs (VACNTs) directly on metallic current collectors or metal underlayers are suggested to have an added advantage of reduced contact resistance [3]. However, detailed and rigorous studies on the contact resistance at CNT-metal interfaces are lacking in the literature. These studies are needed and important for ascertaining design considerations for emerging CNT microelectronic devices.

Understanding the resistance contributions with metal contacts deposited on the top (overlayer) of VACNT arrays is a key objective of the present work. In this study 100 nm of Ti on conductive Si substrate is used as the bottom contact, whereas four different metals (Au, Ti, Al, Ni) are investigated as the top metal contact. Other variables include three different thicknesses for top metal (50, 200, and 500 nm), open and closed tips for VACNTs, and conformal oxide coating of CNTs using Atomic Layer Deposition (ALD) at three different thicknesses (3, 5, and 8 nm) prior to depositing the top metal contact. Electrical characterization was performed by measuring I-V curves with 2-probes and 4-probes using an Agilent E5272A source monitor connected to a DC electrical probing station. The device structure and contact points for electrical characterization are shown in Figure 1 below:

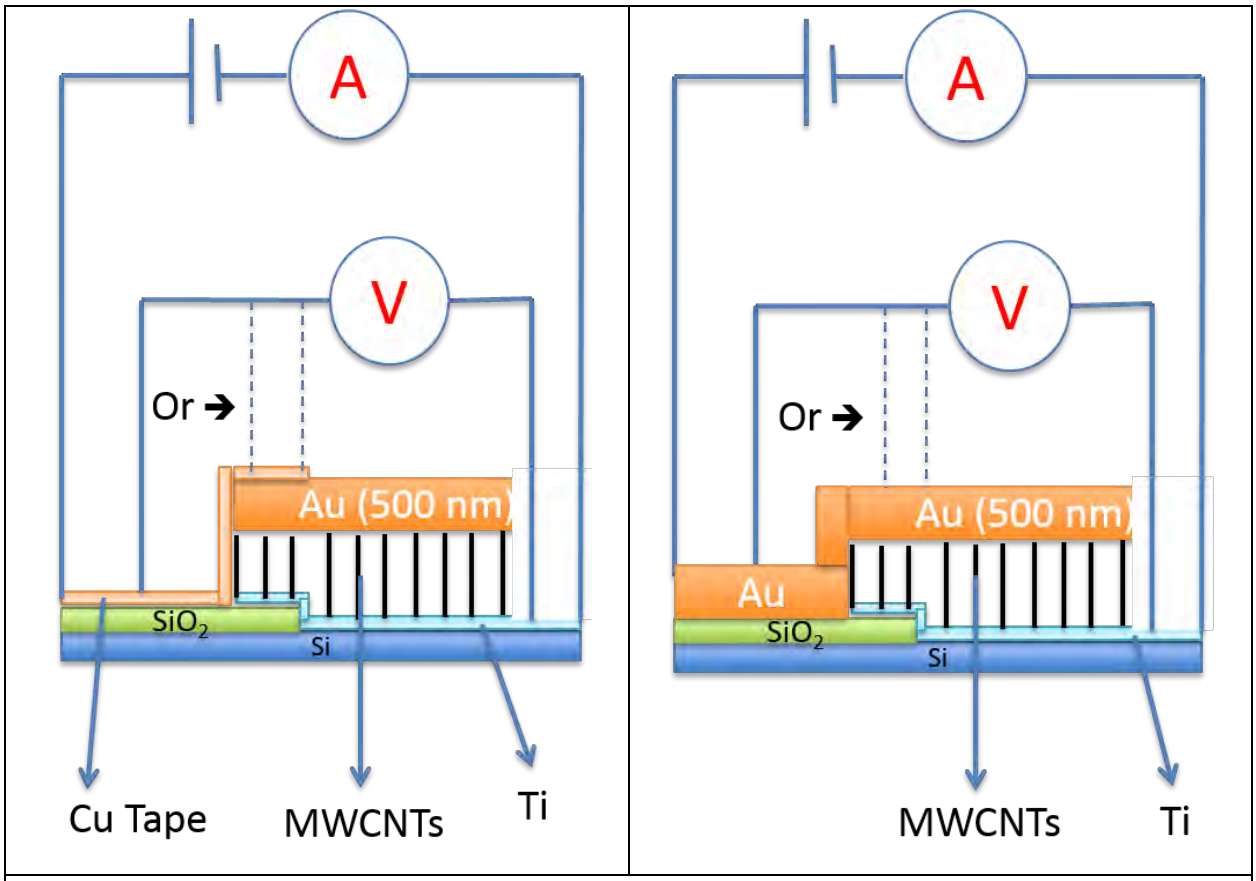

Figure 1: Device structure and probe contact points for 4-probe electrical characterization when (**left**) using Cu tape and (**right**) placing probes directly on top metal. Two-probe measurements were also initially conducted with same configuration except that only one probe was contacted to top and bottom metals, respectively. Contact with bottom metal was made after scraping off the top metal and underlying CNTs over a small section of the sample with rubber-coated tweezers to expose the Ti underlayer. Drawing above is not to scale and probes were placed equidistant from each other for 4-probe measurements.

Preliminary Results:

Two probe electrical measurements with different thickness of Au and Al top metals are shown in Figure 2 and 3. These measurements indicate that there are clear differences in device resistances as a function of the top metal thickness. A thicker top metal layer significantly decreases the device resistance. One explanation might be that the thicker metal top layer decreases porosity in the top metal contact leading to a more continuous conductive overlayer. At lower thicknesses the metal overlayer is more conformal and adapts the same porosity as the VACNT film, which was verified with SEM imaging. Therefore the thicker and more continuous conductive overlayer will reduce the occurrence of electron hopping or tunneling from one metal covered CNT to the next, instead bridging the CNTs with a continuous conductive pathway while reducing interparticle resistances of the VACNT array.

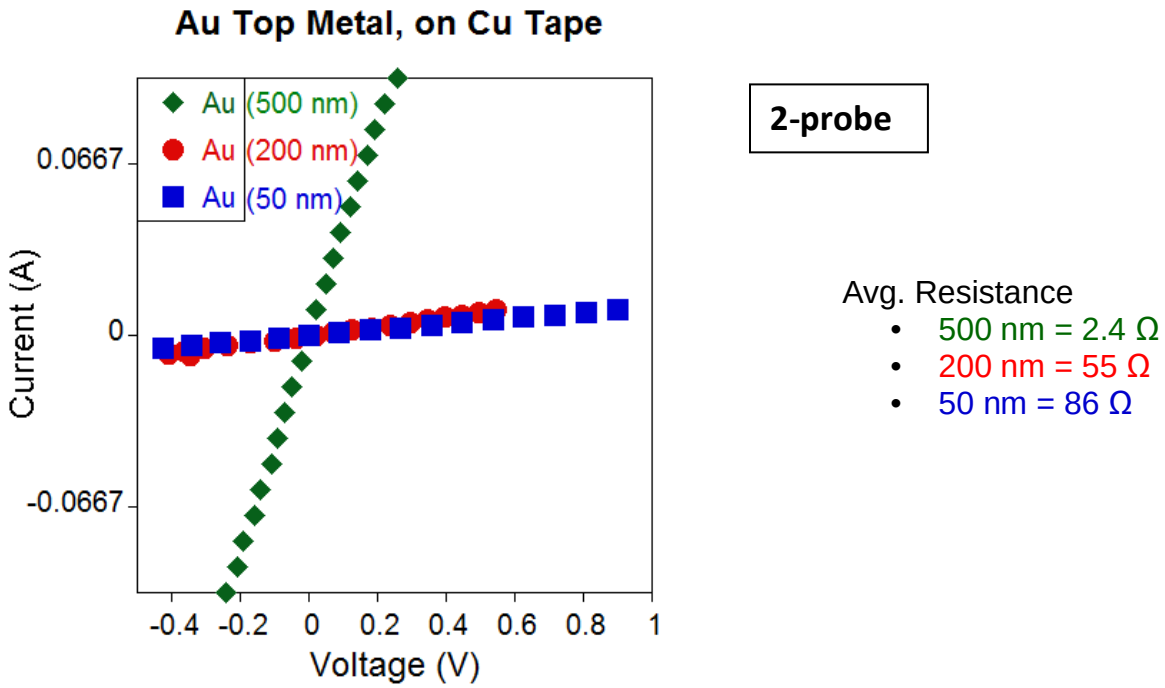

Figure 2. Two-point probe IV curves determined using Cu tape on Au top metal at three different thicknesses. Average resistances from IV curves are displayed on the right.

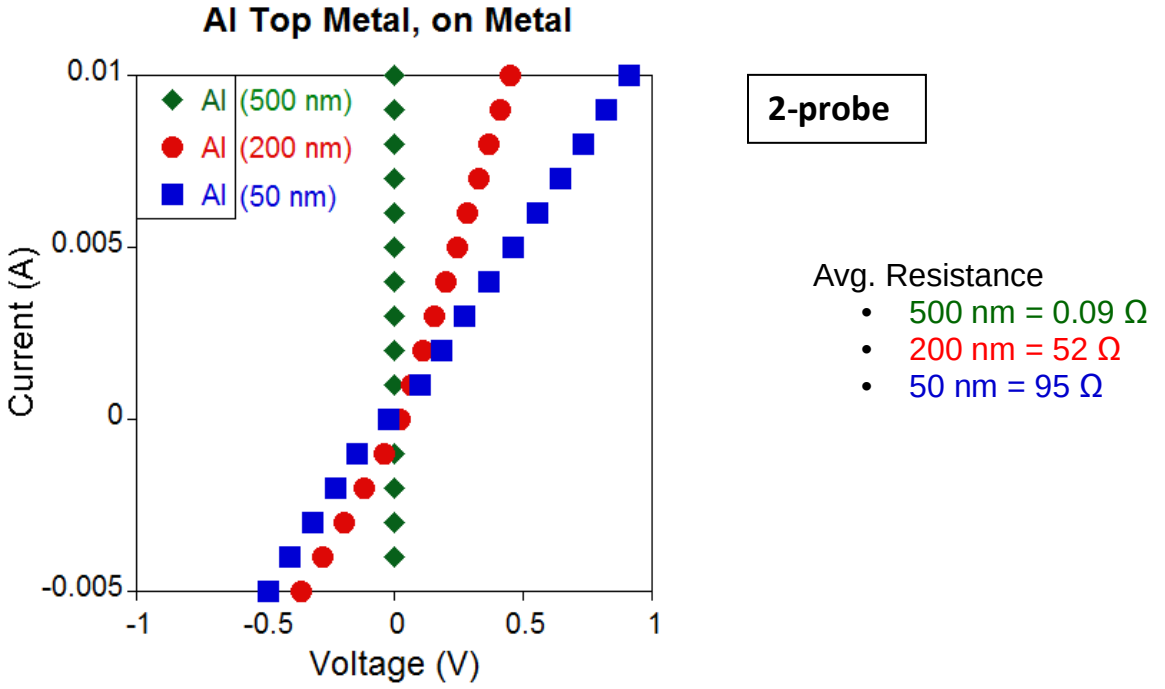

Figure 3. Two-point probe IV curves determined using Al top metal at three different thicknesses. Average resistances from IV curves are displayed on the right.

Two probe electrical measurements across the device for different top metals at constant thickness of 200 and 500 nm are shown in Figure 4 and 5, respectively. These measurements indicate that there are clear differences in device resistances as a function of which top metal is used. It appears that Al and Au top metals result in the lowest device resistance. Although these metals may not wet CNT surfaces as well as Ti metal, their intrinsic resistivity (22 - 28 nΩ m) is much lower than Ti (420 nΩ m) or Ni (69.3 nΩ m) and their wetting properties appear to be sufficient to create a conductive interface.

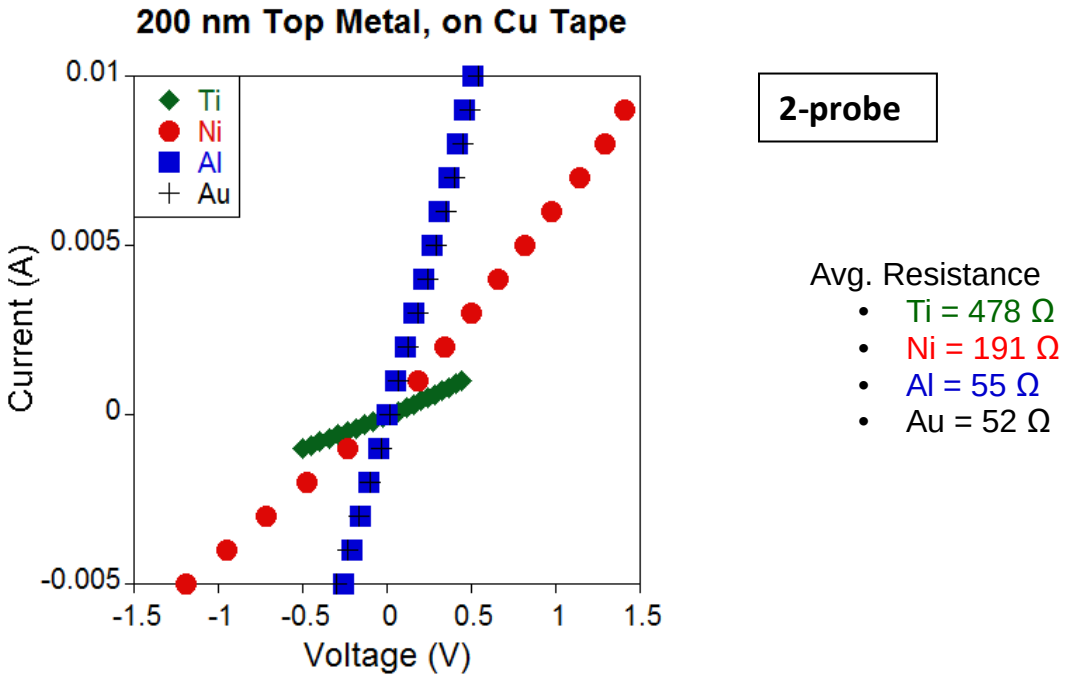

Figure 4. Two-point probe IV curves determined using various 200 nm top metals. Average resistances from IV curves are displayed on the right.

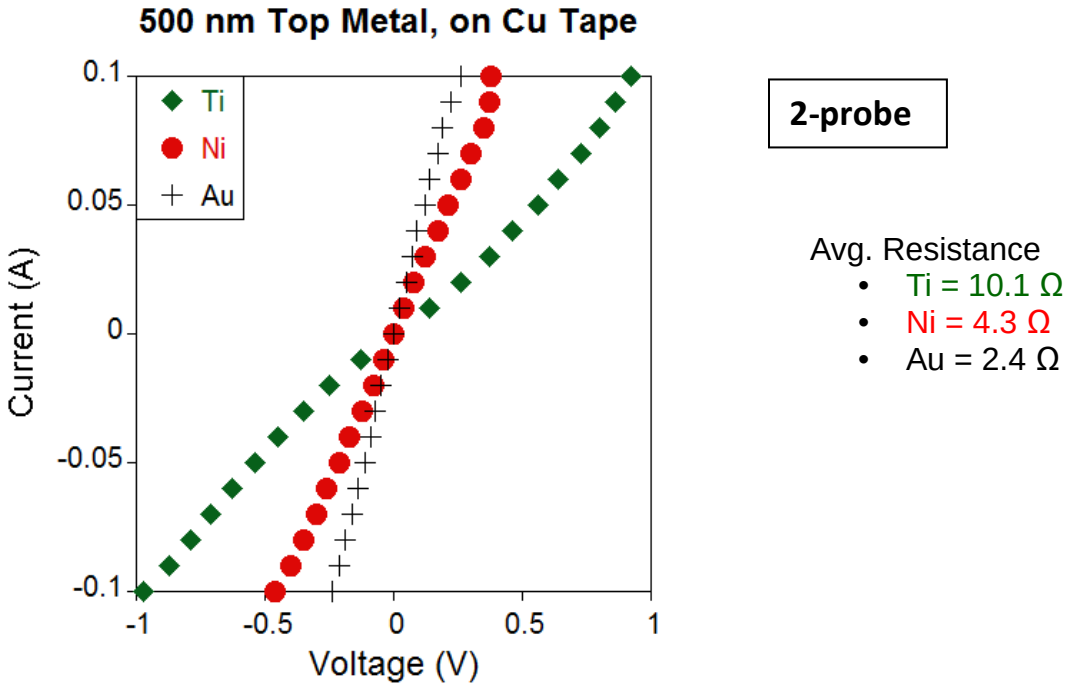

Figure 5. Two-point probe IV curves determined using various 500 nm top metals. Average resistances from IV curves are displayed on the right.

Although two-point probe measurements shown above are appropriate for qualitative comparisons, four-point probe measurements are more accurate for quantitative characterization. Thus, we have transitioned to 4-probe measurements for the remainder of our studies. Nevertheless there are still four configurations for performing the 4-probe electrical characterization measurements as shown in Figure 1. One of our objectives was to determine which configuration was most appropriate for accurate and reliable electrical characterization. Current-voltage characteristics were recorded with all four configurations using a 200 nm Al top metal and results shown in Figure 6. Interestingly, the two configurations using Cu tape as the contact point for probes on the top metal exhibited greater resistances, whereas probes that contact directly with the top metal (Fig. 1(right)) exhibited lower device resistances. This was attributed to the following: Although Cu tape provides a larger area of contact with the metal, it adds two additional conduction interfaces and inherently contains insulating binder as the adhesive thus increasing resistances across the device structure. ***As a result of this data, all future experiments will be done using 4-probes with the testing configuration shown in Fig. 1(right, solid lines), where the top metal is deposited across the entire device and top metal probe contact is made on the metal covered SiO_2 region.***

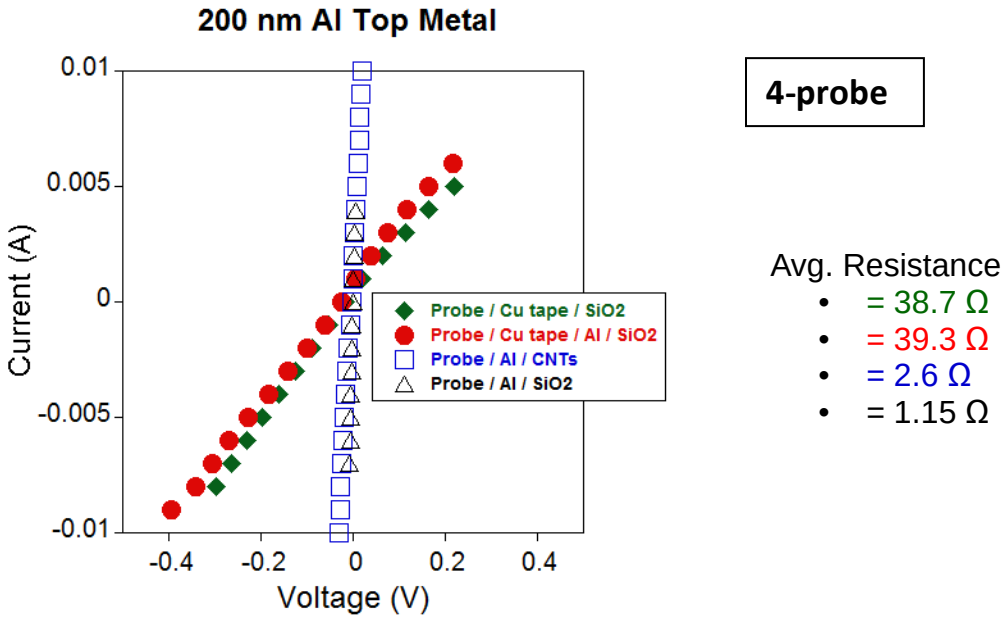

Figure 6. Four-point probe IV curves determined using 200 nm of Al top metal and the four testing configurations shown in Figure 1. Average resistances from IV curves are displayed on the right.

Recent measurements using four-point probe technique with preferred device configuration (i.e. no Cu tape) has revealed that there is no longer a significant difference in device resistance between 200 or 500 nm top metal layer thickness for best performing metals of Au and Al, as shown in Figure 7. Device resistance values are now consistently 1 Ω or less using these metals. In addition, Al may be the best top metal for contacting the VACNT array with closed tips given the lower resistance observed in Figure 7. Although Au has a marginally better conductivity, the Al may be able wet the CNT surface slightly better than Au. Future work is needed to confirm this hypothesis.

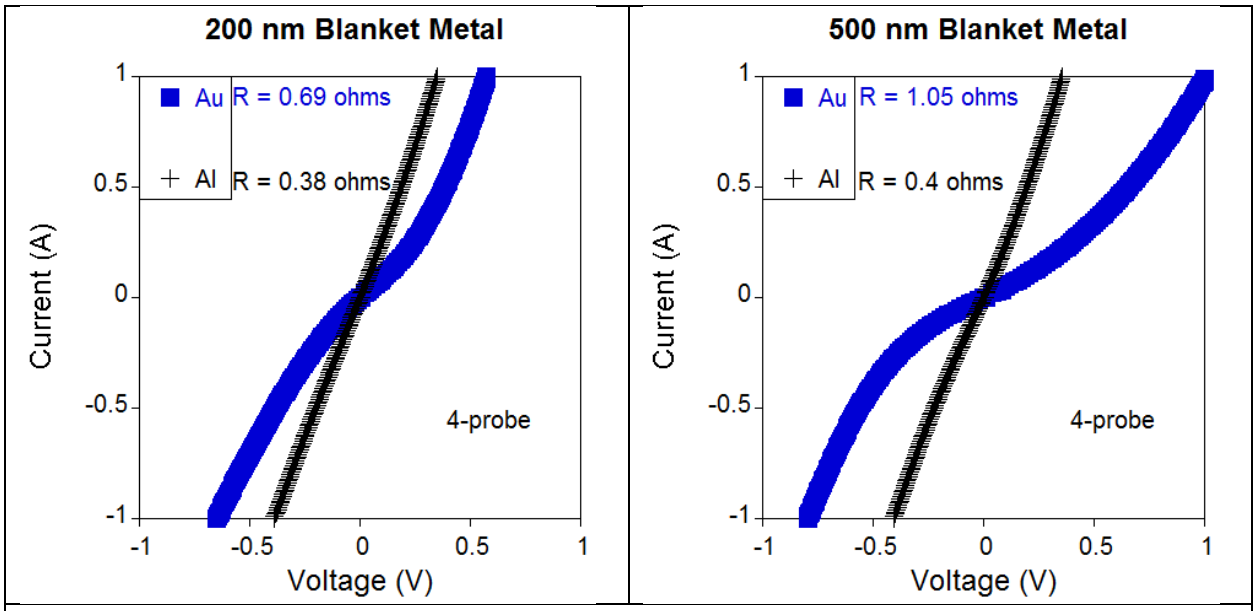

Figure 7. Four-point probe IV curves determined using (left) 200 nm and (right) 500 nm of Au and Al top metal. Average resistances from IV curves are displayed on the upper left.

Future Work:

Now that the methodology for growth and characterization has been determined, below is a 4-phase plan and timeline for future work in order to complete a detailed and rigorous VACNT—Top Metal resistance study on all abovementioned parameters of interest:

PHASE 1:

Samples with Closed Tip CNTs (Total = 36):

Au: 3(50 nm) + 3(200 nm) + 3 (500 nm)= 9 samples

Al: 3(50 nm) + 3(200 nm) + 3 (500 nm)= 9 samples

Ni: 3(50 nm) + 3(200 nm) + 3 (500 nm)= 9 samples

Ti: 3(50 nm) + 3(200 nm) + 3 (500 nm)= 9 samples

(Out of 3 samples for each thickness, one would be used for SEM and 2 for IV characterization)

Outcome: Sample with best thickness and best top metal (one with high work function and one with low) will be identified.

PHASE 2:

Opening CNT Tips (Total = 20):

Etch time 1-5 minutes: 20 samples (changing time and power)

Open tip CNTs samples (Total = 12):

Au:3 Ti:3 Ni:3 Al:3

Outcome: The optimum etch time and plasma power for opening CNT tips will be identified. The top metal with lowest device resistance on open tip CNT arrays will be identified.

PHASE 3:

After selecting open or closed tips:

Oxide (Al_2O_3) coating (Total = 36):

3 nm oxide:	Au:3	Ti:3	Ni:3	Al:3
5 nm oxide:	Au:3	Ti:3	Ni:3	Al:3
8 nm oxide:	Au:3	Ti:3	Ni:3	Al:3

Outcome: Select best oxide thickness

PHASE 4 (FINAL):

After selecting appropriate thickness of Metal, Oxide & open tip(Total = 12):

Au:3 Ti:3 Ni:3 Al:3

Total Samples: 116

Phase 1 : 36 samples (Aug 31, 2015)

Fabrication: 2 weeks

SEM and IV test: 1 week

Phase 2: 32 samples (Sept 15, 2015)

Fabrication: 2 weeks

SEM and IV test: 1 week

Phase 3: 36 samples (Sept 30, 2015)

Fabrication: 2 weeks

SEM and IV test: ½ week

Phase 4: 12 samples (Oct 15, 2015)

Fabrication: 1 week

SEM and IV test: 1 week

Phase 5: **(Oct 31, 2015)**

Paper Draft

Motivation for Research and Development of Optical Rectennas:

The extension of rectennas from the microwave to the IR and visible regimes offers enormous potential benefits [4]. In addition to the breakthroughs in our understanding of basic physics, optical rectennas would be useful in many transformative applications, including photovoltaics (the conversion of photon energy to electrical energy), solar cells (the conversion of solar energy to electrical, thermal, or chemical energy), nanophotonics, near-field optics, IR sensing, and imaging (including medical and chemical sensors). Another increasingly important application is the transmission and reception of information. This is significant since the density of transmitted information is greater at higher frequencies, where the density varies as the square of the frequency. Furthermore, for transmission through the atmosphere, losses decrease as the frequency increases [5, 6].

Recent Literature Trends:

Perhaps in direct proportion to the potential benefits, optical rectification has faced important challenges in materials processing and theoretical understanding. Recent literature has revealed new approaches to fabrication of optical rectennas that avoid performance limitations associated with conventional fabrication approaches for rectenna such as those that employ Schottky Diodes or Metal/Insulator/Metal (MIM) diodes with parallel plate electrodes. Two new optical rectenna fabrication approaches in recent literature include development of (1) Monolithic Nanoscopic Tunnel Junctions (MNTJ) [4], and (2) 2D planar geometric diodes coupled with bow-tie antennas [7].

The MNTJ rectenna is based on metal–vacuum–metal (MVM) tunnel junction gaps that can now be reproducibly fabricated down to ~1 nm with scaled device arrays over cm^2 sized areas using selective ALD. In particular, for Cu, the selective ALD process is self-limiting at gap separations of 1 nm. For gap distances of this size, rectification of radiation with frequencies up to blue portion of the spectrum is possible.

The geometric diode consists of a conducting thin-film, currently graphene, patterned into a geometry that leads to diode behavior. In contrast with MIM diodes that have parallel plate electrodes and are limited in their RC response time and poor impedance matching between diodes and antennas, the planar structure of the geometric diode provides a low RC time constant, on the order of 10^{-15} s, which permits operation at optical frequencies. Optical rectification at 28 THz has been measured from rectennas formed by coupling graphene geometric diodes with metal bowtie antennas.

References:

[1] Y. Ando, X. Zhao, H. Shimoyama, G. Sakai, K. Kaneto, Physical properties of multiwalled carbon nanotubes, Int. J. Inorg. Mater. 1 (1999) 77–82.
[2] B.Q. Wei, R. Vajtai, P.M. Ajayan, Reliability and current carrying capacity of carbon nanotubes, Appl. Phys. Lett. 79 (2001) 1172–1174.
[3] B.R. Stoner, B. Brown, J. T. Glass, Diamond & Related Materials 42 (2014) 49–57.
[4] N. M. Miskovsky, P. H. Cutler, P. B. Lerner, et al., *Rectenna Solar Cells*, Chapter 7: Nanoscale Rectennas with Sharp Tips for Absorption and Rectification of Optical Radiation, (2013).
[5] J. Alda, J. Rico-García, J. López-Alonso, G. Boreman. Optical antennas for nano-photonic applications. Nanotechnology. 16 (2005) S230.
[6] P. Bharadwaj, B. Deutsch, L. Novotny. Optical antennas. Adv Opt Photonics. 1 (2009) 438.
[7] Z. J. Zhu, Graphene Geometric Diodes for Optical Rectenna. Ph.D. Thesis. (2014).

Georgia Tech NEST
NanoEngineered Systems and Transport

Ultrafast Carbon Nanotube-Oxide-Metal Tunnel Diodes for Infrared and Optical Rectenna: A Study of the Limiting Resistances

Interim Progress Report (64600-EL-YIP)

For the Period 15 October 2013 to 31 July 2014

PREPARED B. Cola (404-385-8652)

AGREEMENT NUMBER: W911NF-13-1-0491
DATE SUBMITTED: October 1, 2014

SUBMITTED BY: Georgia Tech Research Corporation
505 10th Street
Atlanta, GA 30332

1.0 Program Summary

The response of a multiwall carbon nanotube to visible light has been reported to be consistent with conventional radio antenna theory.[1] Several researchers have proposed that this result could be exploited to realize an optical rectification device – that is, a device that converts free-propagating electromagnetic waves at optical frequencies to localized direct current energy. However, an experimental demonstration of this concept requires that the multiwall carbon nanotube antenna be coupled to a diode that operates above 430 terahertz (a switching speed on the order of 1 femtosecond). Ultralow capacitance, on the order of a few attofarads, could allow a diode to operate at these frequencies; and the development of metal-insulator-metal tunnel junctions with nanoscale dimensions has emerged as a potential path to diodes with ultralow capacitance, but these structures remain difficult to fabricate and couple to a nanoscale antenna reliably. Here we develop optical rectification by engineering metal-insulator-metal tunnel diodes at the tips of multiwall carbon nanotubes, which act as the antenna and metallic electron emitter in the diode. Diode areas around 10 nm, geometric field enhancement at the carbon nanotube tips, and a low work function semi-transparent top metal contact enable this demonstration. However, device performance is limited by contact resistances, which are the focus of this research program. Using vertically-aligned arrays of the diodes, we measure voltage and current at visible and infrared electromagnetic frequencies that is due to a rectification process, and quantify minor contributions from thermal effects, which depend on metal contacts to CNTs and can obscure a rectification signal if not well understood. **Our efforts during this period of performance focused on** quantifying thermoelectric effects due to contacts to CNTs. We established an experimental setup to make these measurements precisely. We also furthered our general understanding of the effect of resistance on the optical rectification mechanisms in our device. In particular, we discovered that there is a factor of 20 decrease in zero-bias resistance and a loss of non-linearity of the voltage dependence under monochromatic illumination, and that this resistance appears to be the critical one for determining device performance as opposed to the zero-basis resistance determined from the dark current. This is in contrast to a recent report of optical rectification in plasmonic vacuum nanogaps,[2] but in agreement with recent theoretical predictions from Prof. Garret Moddel's group at UC Boulder.[3] The difference in our result may be attributed to the asymmetry in contact metals in our case, which is a subject of ongoing investigation. Interestingly, the resistance change is much less under broadband solar illumination, which suggest that there are important effects of scattering or incoherence that must be considered in this case. During this period we also make initial progress towards optimizing a recipe to open the ends of multiwall CNTs to connect to their inner walls for reduced resistance.

2.0 Program Detailed Technical Progress

2.1 Establishment of New Characterization Lab

The first series of funds was reallocated, after approval from the program manager, to the purchase of equipment to establish a new lab. This was possible because the student on the project could be supported by a fellowship. Establishing this lab was required because the open facilities that we used early in this work were no longer available. Funds were used to purchase and install a probe station, solar simulator, monochrometer, optical table, and LCR and capacitance meters. Figure 1 show one of our rectenna devices tested in the new lab, and Figure 2 shows the full characterization setup on the optical table. With this setup we can measure basic electrical device characteristics including impedance and capacitance as a function of frequency, and rectenna response as a function of incident light wavelength and power. We are very grateful

to the program manager for allowing us to make this modification to the budget to acquire this critical equipment for the program (and hope that he will visit our lab to check it out!).

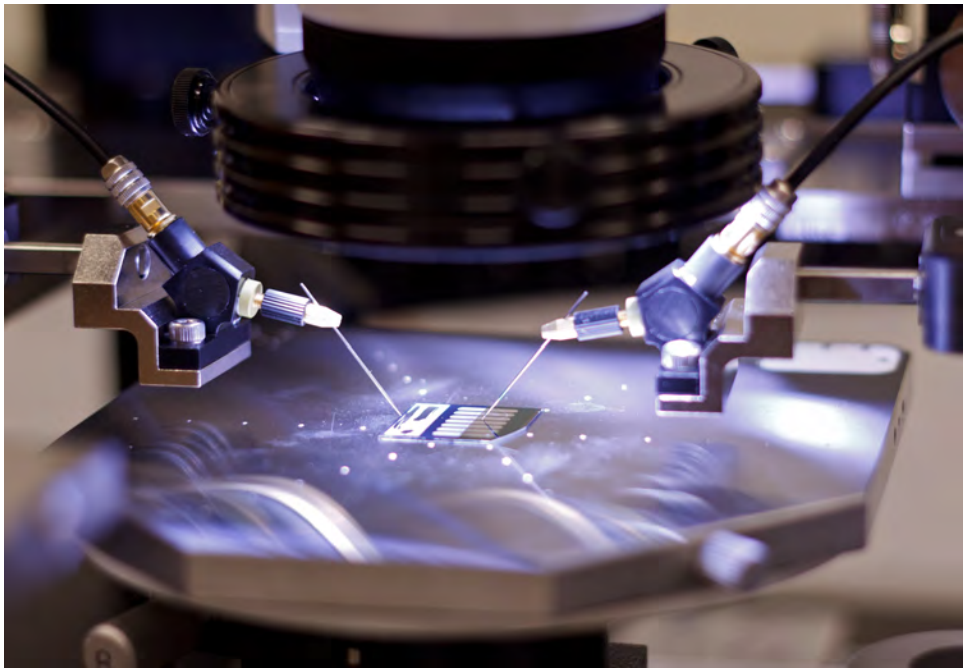

Figure 1. Rectenna device under test.

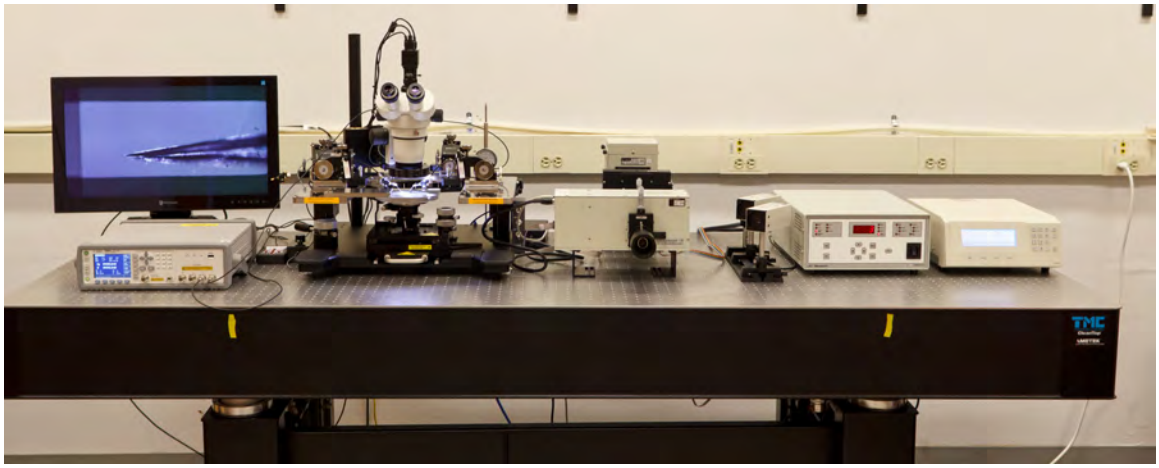

Figure 2. Full lab capabilities. Electrical meters, probe station, and solar simulator with monochrometer.

2.2 Understanding Thermoelectric Effects

Recently, Prof. Junichiro Kono's group at Rice University has shown impressive results for broadband photothermoelectric detectors based on horizontally aligned CNT arrays.[4,5] Fundamental to their device operation is the existence of a thermoelectric effect in the single-wall CNTs, and their ability to establish a substantial thermal gradient across the device, which is on the order of 1 mm in length. Since the thermal voltage scales proportionally to the magnitude of the thermal gradient, and the long length of their devices enables a large thermal gradient, the devices from Kono's group can produce voltages on the order of 1 mV due to a thermoelectric effect.

Because the magnitude of voltage produced by our CNT rectenna devices is on the order of 1 mV, the result published by Kono caused us to take a second look at the thermal behavior of our devices. In contrast to Kono's devices, our devices span only ~ 10 microns between metal contacts (as opposed to 1 mm). Because of the very short distance between metal contacts in our devices it is unlikely that our devices can produce a thermoelectric voltage on the order of the rectenna responses we have measured, but we proceeded during this phase of the effort to answer this question clearly and quantitatively.

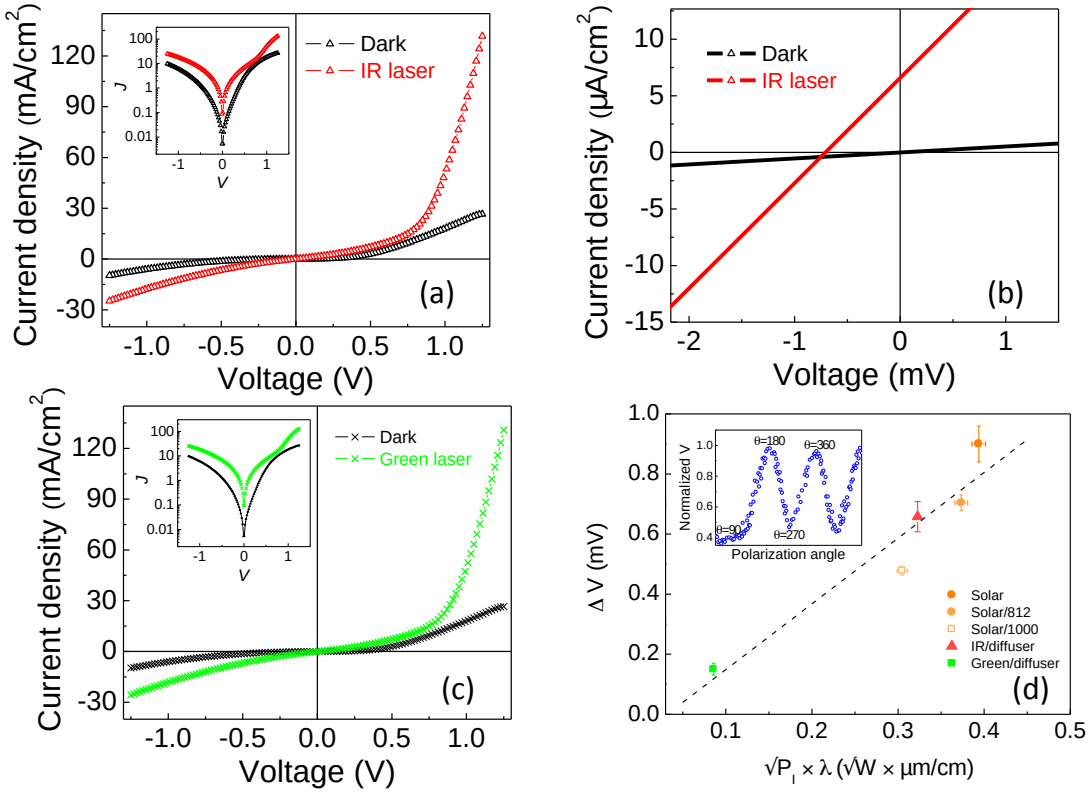

Figure 3. (a) Current-voltage characteristics in dark and 1064 nm light. (b) Close up of part (a). (c) Current-voltage characteristics in dark and 532 nm light. (d) Voltage scaling with classical antenna effects for 532 nm (26 mW/cm^2), 1064 nm (92 mW/cm^2), and simulated solar illumination (100 mW/cm^2) with different levels of power filtering. The inset shows the polarization dependence of the voltage.

It is useful to first recall in Figure 3 that our devices produce rectified voltages on the order of 1 mV with a maximum illumination intensity of 100 mW/cm^2. Also note that the illuminated I-V curve shows a change in non-linearity, which is not observed in a thermoelectric response[4,5] where a linear I-V shifts up magnitude without loss of linearity. So this fact is the first evidence against a significant thermoelectric effect in our devices. To address the question of what is the order of magnitude of a thermoelectric voltage in our devices, we conducted systematic experiments as illustrated in Figure 4.

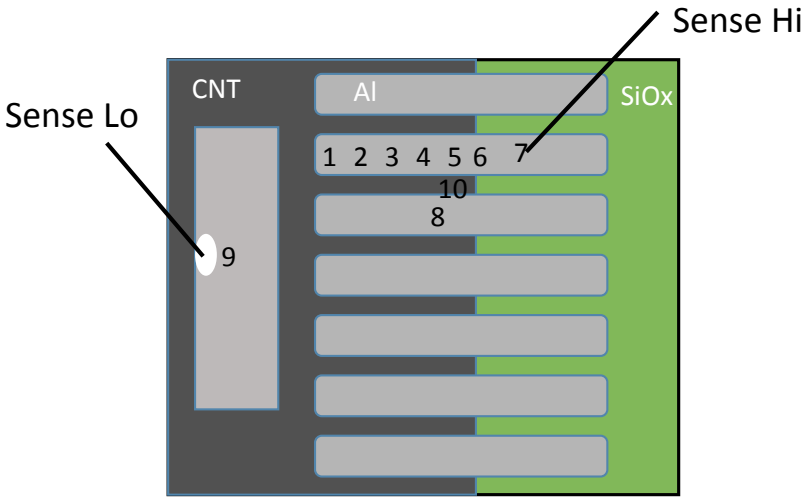

Figure 4. Illustration of the structure of our rectenna devices. The Al contact metal is 200 nm thick to be opaque and prevent an optical rectification response, so the measured responses are due to thermal effects. The samples are heated with 236 mW/cm^2 532 nm laser intensity, which is about 2.4 times more intense than the maximum intensity in our rectenna response test. Sense Lo and Hi are where the probe tips make contact. Numbers on the diagram correspond to position values in the plot in Figure 5. Moving the heating from close to the Hi to the Lo probe tip flips the polarity of the voltage, which is a strong indication of a thermoelectric voltage. Voltage at position 7 is at the background level indicating that the thermoelectric effect is not from the probes.

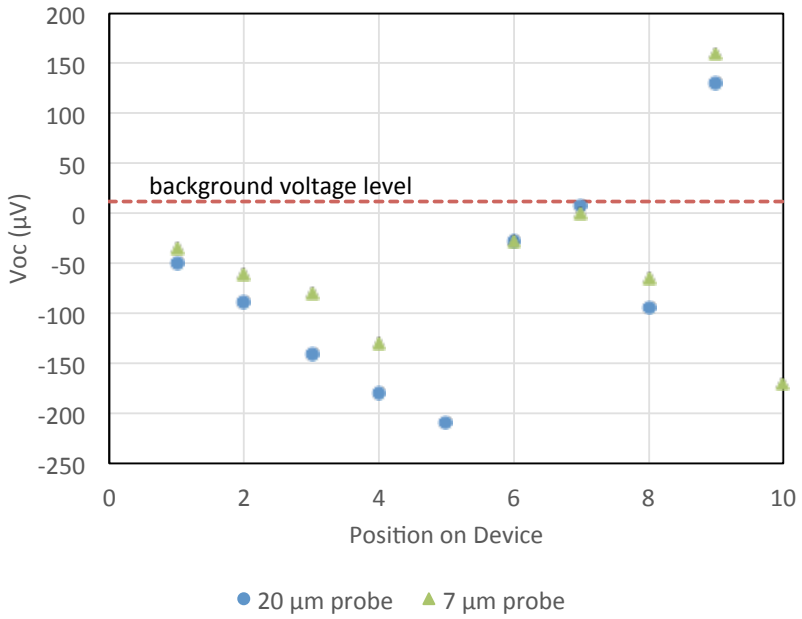

Figure 5. Voltage response due to thermoelectric effects, heated with 236 mW/cm^2 532 nm laser intensity, which is about 2.4 times more intense than the maximum intensity in our rectenna response test. The rectenna response is ~ 1 mV.

Figure 5 shows that the larges thermoelectric voltage produced in our devices is about 0.2 mV at about 2.4 time the intensity, which means that the thermoelectric voltage is at least an order of magnitude lower than the rectenna response in our devices.

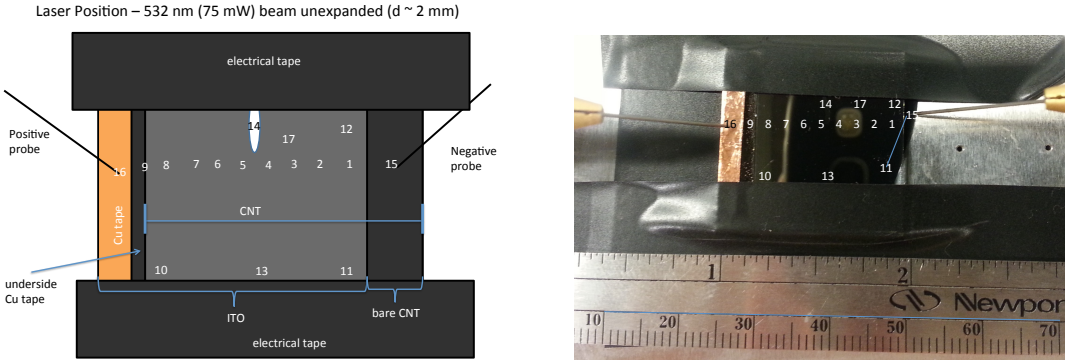

Figure 6. Metal-CNT-oxide-ITO stack used for thermoelectric effect testing.

To explore the thermoelectric effects in our devices further, we made “dry contact” samples using indium tin oxide (ITO) on glass in physical contact with oxide-coated CNT arrays. This stack is interesting because it is on our roadmap for a potentially simpler device structure. Figure 6 shows the test setup for this device structure, with similar labeling of the laser heating locations as in Figures 4 and 5 to map the thermoelectric effect. Figure 7 shows the voltage mapped as a function of distance from the negative probe, which is contacting the Ti layer below the CNTs. The positive probe is contacting the Cu tape on the ITO (as shown in Figure 6), which is in dry contact with the oxide-coated CNT tips. The fact that the voltage in Figure 7 changes sign at the half way point between the positive and negative probes is a strong sign that the response is due to a thermoelectric effect, which is again about an order of magnitude smaller than our rectenna response voltage.

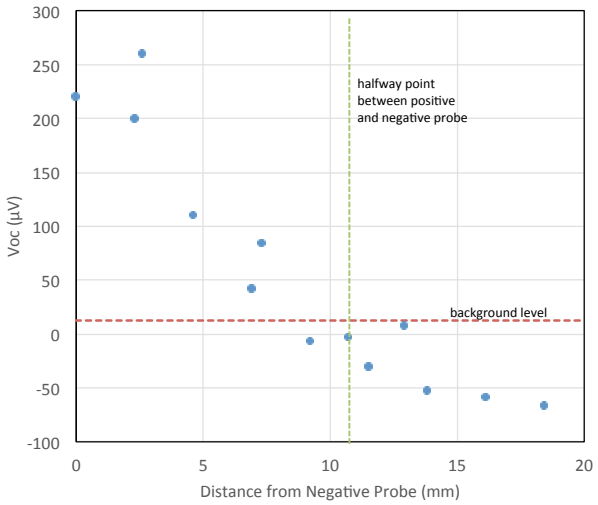

Figure 7. Thermoelectric voltage vs. distance for the sample stack in Figure 6.

2.3 Understanding the Dynamics of Diode Resistance

Typically the dark current-voltage is used to compute diode resistance,[2] responsivity, and other important performance characteristics. However, this approach assumes that the diode resistances change with voltage in a constant way during device operation. This assumption breaks down in tunnel diodes when they are illuminated with photons that are energetic enough to contribute to the tunneling process – that is, photon-assisted tunneling. There is a well-established semi-classical correction[6] to consider photon-assisted tunneling, but this expression has not been confirmed experimentally at optical wavelengths. We measure drastic changes in the resistance of our diodes when illuminated that do not agree with established theory quantitatively. However, the results do agree with the general trends predicted by the theory,[3] that is, that the resistance and responsivity of our diodes decrease under illumination. Figures 8-10 show the dark and light zero-basis resistance for the same device, illuminated by 1064 nm, 532 nm, and full simulated solar. The resistance decreases by about a factor of 20 for the monochromatic illumination cases and losses its non-linear characteristic, but barely changes under broadband solar illumination. This could be due to the multiple wavelengths/photon energies contributing to scattering or phase cancelation effects in the rectenna. Also the fact that we have CNTs and Ca as asymmetric metals on both sides of the oxide could cause changes in diode performance due to changes in the local electron distributions. But the fundamental origin of these effects is a point of continued investigation.

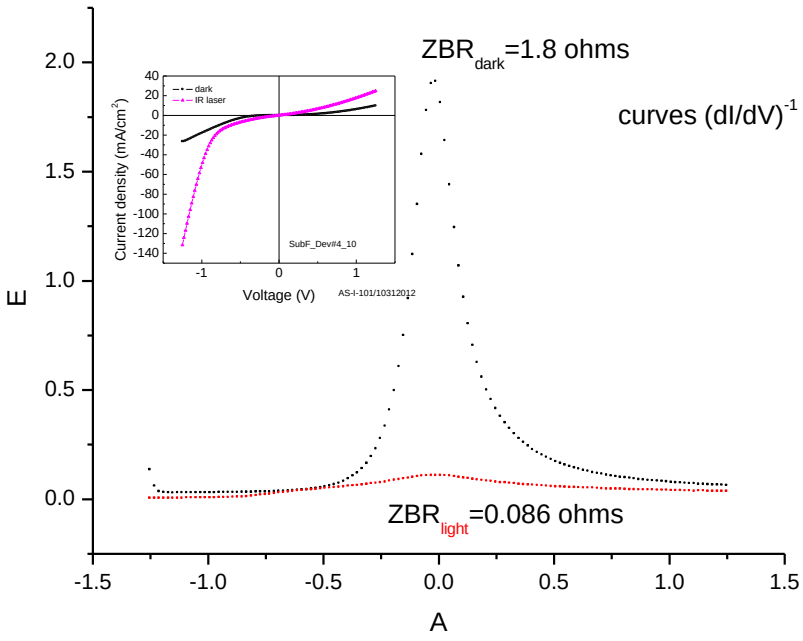

Figure 8. Dark and light differential resistance for 1064 nm illumination of CNT rectenna device.

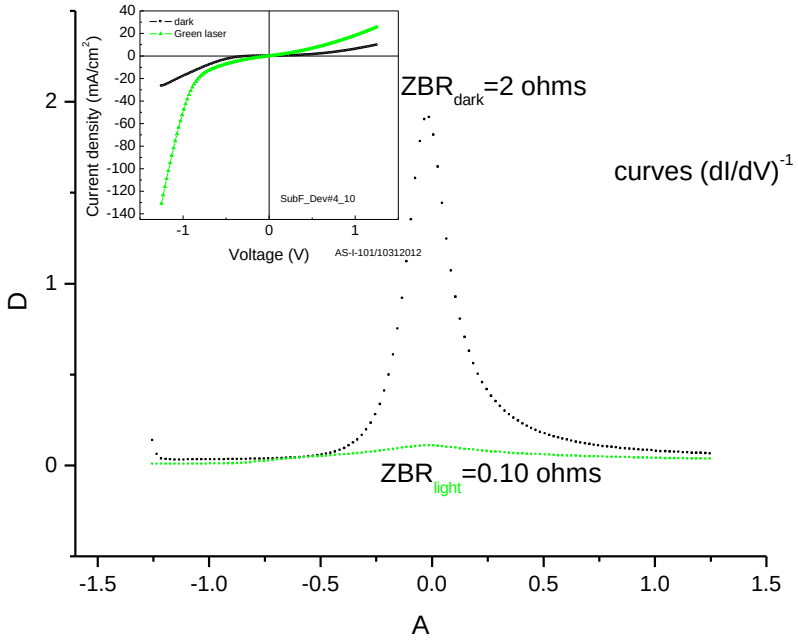

Figure 9. Dark and light differential resistance for 532 nm illumination of CNT rectenna device.

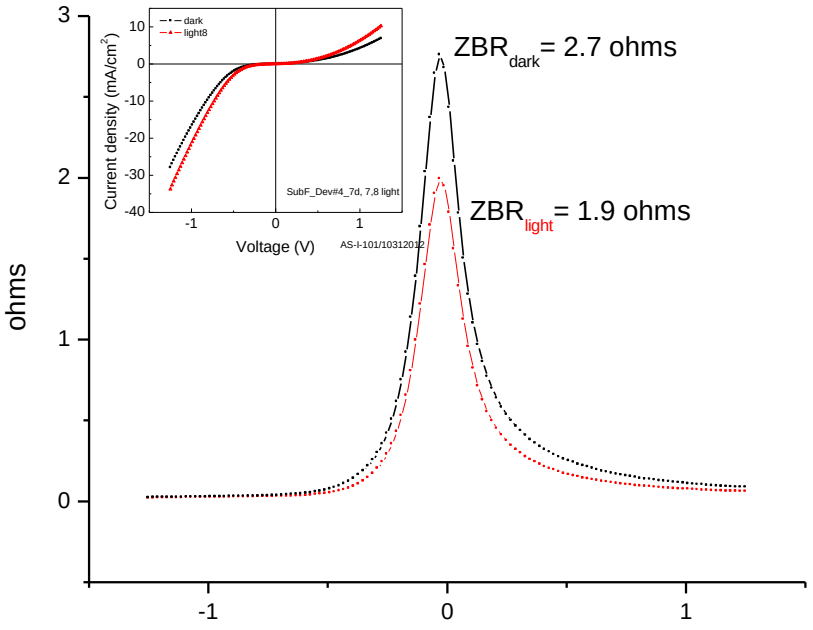

Figure 10. Dark and light differential resistance for full simulated solar illumination of CNT rectenna device.

A consequence of the reduced non-linearity of the diodes under monochromatic illumination is a loss in diode sensitivity or responsivity. The rectified voltage is proportional to the sensitivity[7] so this loss will ultimately reduce the efficiency of the energy rectification and measures should be explored to counter it. Figure 11 shows the responsivity of our diode under 523 nm, 1064 nm, and simulated solar illumination. The dark current responsivity is shown for comparison. Both the dark and solar responsivity at zero bias is approximately 2 A/W. The responsivity under the two laser illumination cases is around 0.1 A/W. Further testing is required to fully understand the changes in the responsivity magnitude and shape of curve under laser illumination.

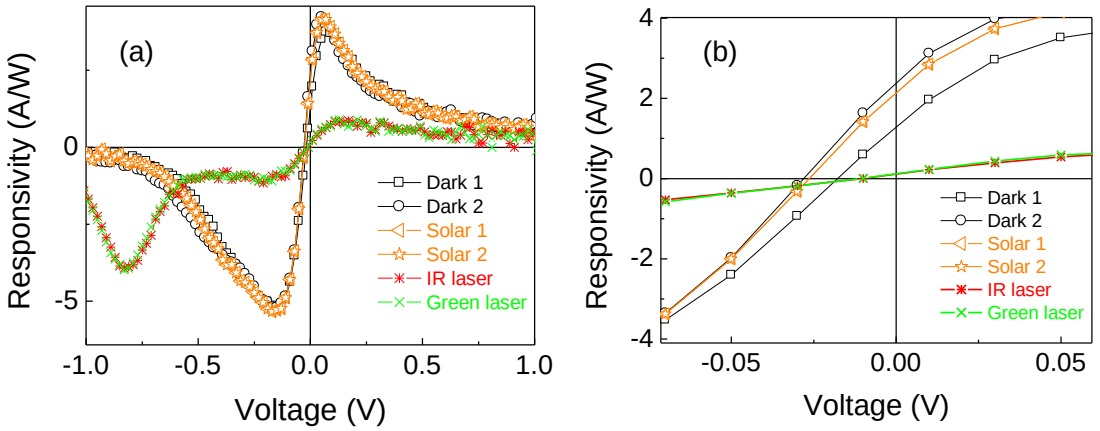

Figure 11. (a) Responsivity of CNT rectenna under 523 nm, 1064 nm, and simulated solar illumination. (b) Close up of (a).

2.4 Towards Contact to Inner Multiwall CNT Walls

We began developing a direct RF-plasma process for etching the tips of multiwall CNTs to enable metal contact to all walls. A Uniaxis reactive ion etch tool was used with 10 sccm O_2, 75 mTorr, RF power 80 W, DC bias 245V, and 30 seconds etch time. Figure 12 shows clear evidence of CNT etching after 30-second plasma treatment. Transmission electron microscopy (TEM) studies are in progress to examine the efficacy of this process to open the CNT ends and expose the inner shells. The process will be optimized based on the information gained from TEM.

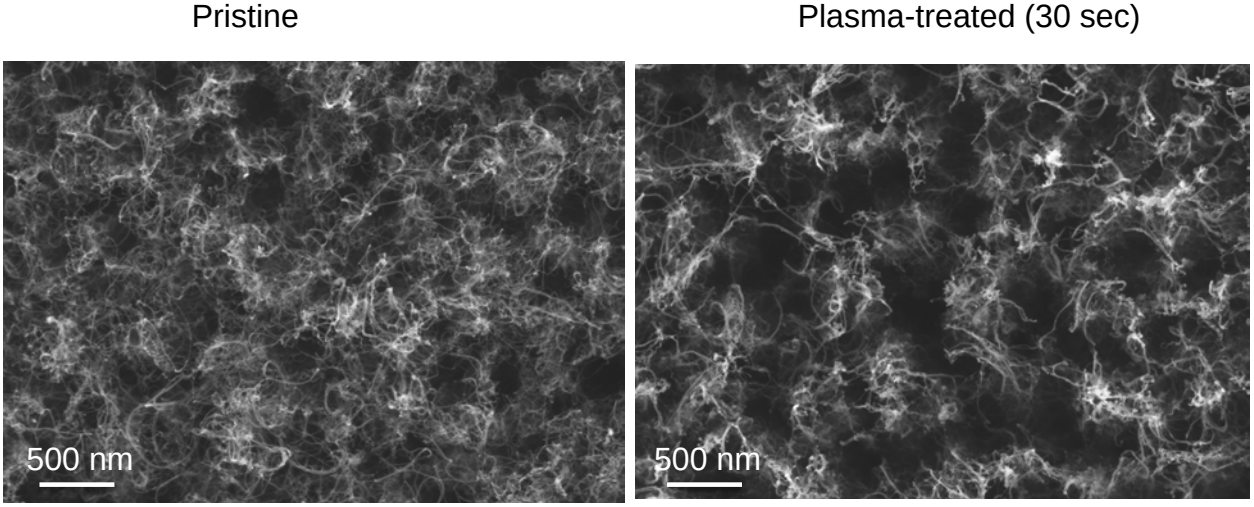

Figure 12. Scanning electron micrographs of CNTs (top view) before and after plasma etch to open CNT end caps.

3.0 Summary, Conclusions and Challenges

In this period we were able to build from scratch a new lab for characterizing rectenna devices. The measurement systems were carefully calibrated on standard samples. We were able to quantify thermoelectric effects and show that they are not responsible for the photoresponse of our devices in a detailed way. We revealed interesting changes in diode resistances under illumination, which depend on if the light is monochromatic or broadband. The non-linearity of the diodes also reduces under monochromatic illumination, which reduces the sensitivity of the devices. We believe that these results will require modification of existing theory to ultimately explain the relation between diode resistance and the mechanisms of rectification. Finally, we began development of a process to etch and open the end caps on CNTs to enable further studies where we will deposit metal and quantify how this processing affects contact resistances. Based on our results that unambiguously confirm optical rectification in our CNT tunnel diodes, we have drafted a manuscript that we plan to submit to *Nature* within the month.

One major challenge faced during this period was our inability to access proper equipment for depositing low work function metals as top contacts – that is, a metal thermal evaporator with a long working distance that is also connected to a glove box. Such a tool is required for the deposition of metals like Ca that are very reactive in air, and in general to prevent the metals from diffusing into the oxide at high temperatures, which produces device shorts. Prior to the start of this program we were accessing a tool in another researcher's lab for this processing. But access to this tool has become difficult. To address this problem that is hampering our progress we plan to submit a DURIP proposal to acquire a metal deposition system to install in our lab for controlled processing.

4.0 References

1 Jensen, K., Weldon, J., Garcia, H. & Zettl, A. Nanotube Radio. *Nano Letters* **7**, 3508-3511, doi:10.1021/nl0721113 (2007).

2 Ward, D. R., Huser, F., Pauly, F., Cuevas, J. C. & Natelson, D. Optical rectification and field enhancement in a plasmonic nanogap. *Nat Nano* **5**, 732-736,

doi:http://www.nature.com/nnano/journal/v5/n10/abs/nnano.2010.176.html -supplementary-information (2010).

3 Sachit, G., Saumil, J. & Garret, M. Quantum theory of operation for rectenna solar cells. *Journal of Physics D: Applied Physics* **46**, 135106 (2013).

4 He, X. *et al.* Carbon Nanotube Terahertz Detector. *Nano Letters* **14**, 3953-3958, doi:10.1021/nl5012678 (2014).

5 Nanot, S. *et al.* Broadband, Polarization-Sensitive Photodetector Based on Optically-Thick Films of Macroscopically Long, Dense, and Aligned Carbon Nanotubes. *Sci. Rep.* **3**, doi:http://www.nature.com/srep/2013/130226/srep01335/abs/srep01335.html -supplementary-information (2013).

6 Tien, P. K. & Gordon, J. P. Multiphoton Process Observed in the Interaction of Microwave Fields with the Tunneling between Superconductor Films. *Physical Review* **129**, 647-651 (1963).

7 Gadalla, M. N., Abdel-Rahman, M. & Shamim, A. Design, Optimization and Fabrication of a 28.3 THz Nano-Rectenna for Infrared Detection and Rectification. *Sci. Rep.* **4**, doi:10.1038/srep04270 (2014).